Appendix C – Carrying capacities definition

Erwan Ike de Bantel[a,*], Thibault Pirson[b], Gonzalo Puig-Samper[c], Jan Marcus Hartmann[d], David Bol[b], Ghada Bouillass[a], Bernard Yannou[a], Marija Jankovic[a], Michael Hauschild[e,f]

[a] *Université Paris-Saclay, CentraleSupélec, Laboratoire Genie Industriel, 91190 Gif-sur-Yvette, France* [b] *ICTEAM, Université catholique de Louvain, Louvain-la-Neuve, Belgium* [c] *Luxembourg Institute of Science and Technology, 5 Avenue des Hauts-Fourneaux, Esch-sur-Alzette, L-4362, Luxembourg* [d] *Institute of Technical Thermodynamics, RWTH Aachen University, Schinkelstraße 8, 52062 Aachen, Germany* [e] *Section for Quantitative Sustainability Assessment, Department of Environmental and Resource Engineering, Technical University of Denmark, 2800 Kgs. Lyngby, Denmark* [f] *Centre for Absolute Sustainability, Technical University of Denmark, 2800 Kgs. Lyngby, Denmark*

[*] *Corresponding author: erwan.de-bantel@centralesupelec.fr.*

Contents

Funding Information: The work of Erwan Ike de Bantel received organizational support of the "CircularIT Alliance" project. The work of Thibault Pirson is part of the SOIL project, which received funding from the European Union's Horizon Europe research and innovation program under the HORIZON-KDT-JU-2023-1-IA grant agreement N°101139785. Views and opinions expressed are however those of the authors only and do not necessarily reflect those of the European Union or CHIPS. Neither the European Union nor the granting authority can be held responsible for them.

1 Definition of the concept of carrying capacity

The **carrying capacity** is defined in [Bjørn et al., 2025] as the maximum continuous burden that the environment can sustain without taking critical damage, where *critical damage* indicates that some environmental damage is compatible with sustainable development, but only up to a critical level [Bjørn et al., 2025]. This can also be expressed as the maximum sustained environmental intervention a natural system can withstand without experiencing negative changes in structure or functioning that are difficult or impossible to revert [Bjørn and Hauschild, 2015]. Environmental burden can be expressed at different points in an impact pathway, depending on the environmental indicator (typically 'midpoint').

In practice, carrying capacities are operationalized through the selection of environmental control variables and the definition of associated thresholds. The estimation of the carrying capacities is hence closely related to the LCIA method selected for the characterization of elementary flows in LCA [Bjørn et al., 2025]. In fact, the JRC AESA Guidance (beta version) [Bjørn et al., 2025] reminds that "when sourcing the list of carrying capacity values from the scientific literature, the practitioner should ensure that they were developed for the same impact assessment framework that were used for quantifying environmental burdens and that there is a match between the indicators and units, and not only between the names of impact categories". This is meant to ensure consistency and compatibility in the underlying environmental mechanisms considered. **The two most common approaches used in the literature for the definition of global *static* carrying capacities** are (i) the original PB framework definition [Richardson et al., 2023, Steffen et al., 2015], and (ii) global carrying capacities based on conventional existing LCIA methods such as EF [Sala et al., 2020] or ReCiPe 2016 [Gebara and Laurent, 2023].

The first approach (*PB to LCIA*) adapts LCIA metrics to the planetary boundaries framework by developing specific impact assessment models, i.e., the PB-LCIA method[1] developed by [Ryberg et al., 2018] and expanded by [Galán-Martín et al., 2021, Vázquez et al., 2023, Yang and Paulillo, 2026].

On the contrary, the second approach (*LCIA to PB*) translates the planetary boundaries into LCIA metrics to develop LCIA-based planetary boundaries, coherently with the impact assessment modelling underpinning each category [Sala et al., 2020].

Both approaches have their pros and cons. Although the PB-LCIA approach shows advantages in terms of results interpretation (already aligned with PB categories), it is also a new LCIA method for the LCA community (new characterization factors), which is therefore perceive as less robust than well-known LCIA method such as EF for instance. Carrying capacities definitions[2] for both approaches are provided below, as they are both supported in the UNCASExt framework.

[1] Given that traditional LCIA-methodologies (e.g., EF or ReCiPe) cannot directly be used to evaluate the planetary boundaries [Lund et al., 2025], a set of characterization factors was developed by [Ryberg et al., 2018], referred to as the PB-LCIA method. As explained in [Lund et al., 2025], "the PB-LCIA methodology operationalizes the PBs within a LCA framework by defining characterization factors (CF) for the 85 main elementary flows. Though, the boundaries Biosphere integrity and Novel entities are not considered due to the lack of control variables or because their control variables are considered immature".

[2] Note that the concept of carrying capacity is a broader than concept of planetary boundary, as pointed out by the authors of [Lund et al., 2025]. In fact, a key difference is that the PB framework is a *precautionary framework*, while the carrying capacities attempt to estimate the maximum sustained environmental intervention a natural system can withstand without experiencing negative changes in structure or functioning that are difficult or impossible to reverse.

2 Global carrying capacities from the planetary boundaries framework

The planetary boundaries (PB) framework is nowadays increasingly used in scientific and grey literature, and policymaking. According to authors of [Ryberg et al., 2018, Galaz et al., 2012], this is mostly explained by the fact that (i) it captures multiple global environmental pressures within one integrated framework, and that (ii) it offers quantitative targets (boundaries) to support decision making and action. Furthermore, these boundaries are defined based on best available science and (in principle) neutral towards human values since the PB framework does not specify the mechanisms for staying within the *safe operating space* [Ryberg et al., 2018, Biermann, 2012]. However, the authors of [Dao et al., 2018] explain that in practice, several types of sources have been used to identify the global boundaries, mainly because of different levels of scientific understanding on the issues covered by the PB framework. This section therefore explains the basic concepts underlying the PB framework and how it is used to define carrying capacities, given that the PB framework is increasingly referred to for defining global carrying capacities.

2.1 Overview of the planetary boundaries framework

The PB framework is based on the biophysical and biochemical systems and processes known to regulate the state of the planet [Richardson et al., 2023]. The framework defines a set of biophysical boundaries for key Earth systems processes that human impacts should stay within to maximize the probability of staying in a Holocene-like state, and thereby avoid potentially unacceptable Earth system changes [Steffen et al., 2015, Rockström et al., 2009b]. The Holocene state of Earth is taken as the benchmark reference, as many of the components comprising the planetary boundaries framework were rather stable during this post-glacial geological period spanning the last ten to twelve thousand years [Richardson et al., 2023]. One of the main assumption underlying the framework is that the Earth system stability observed during the Holocene period is a key condition to support life systems conducive to the human welfare and societal development. All boundaries therefore adopt preindustrial Holocene conditions as a reference for assessing the magnitude of anthropogenic deviations [Richardson et al., 2023].

The PB framework gathers nine distinct planetary boundaries, all targeting very different biophysical, biochemical systems and processes. They are defined at the global scale, although some of them have also definition at regional/local scale [Dao et al., 2018]. Each PB is quantified through the use of control variables, which are physical positive quantities used to evaluate the effect on response variable, as shown in Figure 1(b). PB control variables are located at different locations on the impact pathway, as defined by the Driver-Pressure-State-Impact-Response (DPSIR) framework [Bjørn and Hauschild, 2015]. In fact, some control variables are defined at the state level (e.g., atmospheric CO_2 concentration, forest cover) whereas others are defined at the pressure level (e.g., land use change, biogeochemical flows) or the impact level (e.g., climate change, biodiversity loss), as highlighted in [Hellweg et al., 2023, Vea et al., 2020, Bjørn and Hauschild, 2015, Lind and Andersen, 2024]. This is illustrated in Figure 1(c).

Among all planetary boundaries, two are identified as *core* boundaries, i.e., climate change and biosphere integrity as highlighted in Figure 1(a). This means that they have not only a very important impact regarding the state of the Earth system, but also a relatively high impact on the behavior of other PBs. This is one of the reason why there is often a focus on the climate change boundary. In the PB framework, two boundaries are proposed for climate change with two different control variables, i.e., radiative forcing and atmospheric CO_2 concentration. As explained by [Gebara and Laurent, 2023], radiative forcing (set to 1 W/m^2) is regarded as more "inclusive" in its addressing of climate change given that it includes all greenhouse gases (GHG) emissions. The second boundary only relates to atmospheric CO_2 concentration (set to 350 ppm). It is important to highlight that these two different control variables lead to two different planetary boundaries, although they both aims at capturing the impact on climate change.

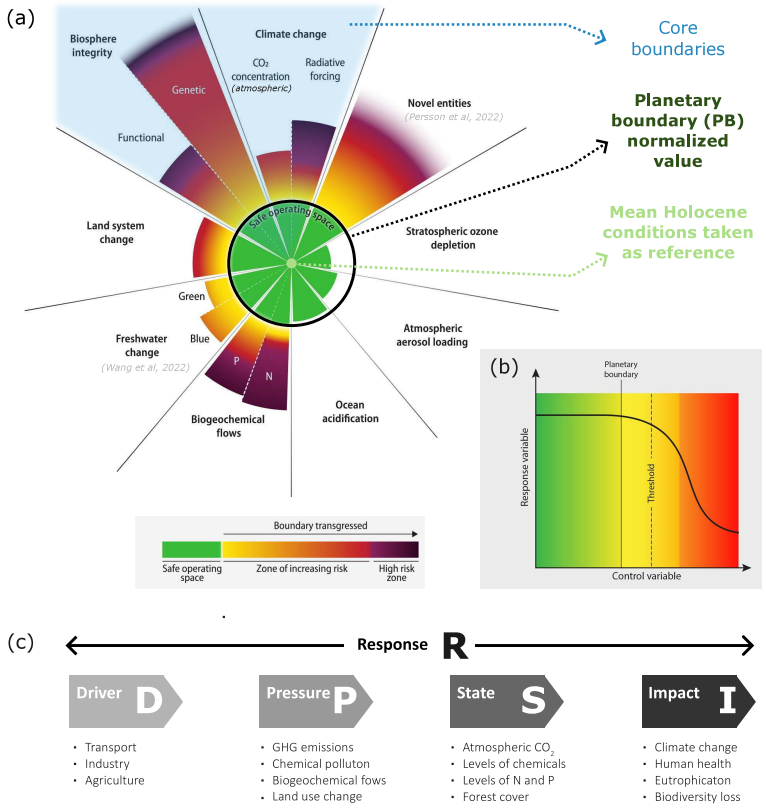

Figure 1: (a) Overview of the planetary boundaries (PB) framework. Caption from the original figure [Richardson et al., 2023] details that the green zone is the safe operating space (below the boundary), yellow to red represents the zone of increasing risk, and purple indicates the high-risk zone where interglacial Earth system conditions are transgressed with high confidence. Values for control variables are normalized so that the origin represents mean Holocene conditions and the planetary boundary lies at the same radius for all boundaries [Richardson et al., 2023]. (b) Conceptual definition of the planetary boundary definition below the threshold, quantified through the control variable. (c) Location of control variable on the impact pathway according to the DPSIR framework [Bjørn and Hauschild, 2015]. Figure and caption adapted from [Richardson et al., 2023, Steffen et al., 2015, Lind and Andersen, 2024].

Since the first publication of the PB framework [Rockström et al., 2009a], several updates have been published to revise it [Steffen et al., 2015, Richardson et al., 2023, Sakschewski et al., 2025]. Aside from updating the current values for each control variable, notable updates[3] include the revision of the planetary boundary for ocean acidification to 2.86-2.75 Ω_{arag} in [Sakschewski et al., 2025] (corresponding to 80-70% of the newly-updated preindustrial Ω_{arag}), and the change of control variable for rate of biodiversity loss to human appropriation of net primary production (NPP) expressed as as fraction of pre-industrial NPP [%]. In the last update of the PB framework, the Planetary Health Check (2025) report concludes that seven of the nine planetary boundaries have been breached, with all of those seven showing trends of increasing pressure [Sakschewski et al., 2025]. This suggests further destabilization of planetary health in the near future, leading to an increasing risk of exceeding so-called tipping points that may lead to irreversible cascading effect [Lejeune et al., 2026].

[3] All details regarding the last updates of the PB framework ca be found in the Planetary Health Check (2025) full report, Table 3 pp.130-131 [Sakschewski et al., 2025]. Updated values are compared to previous values from [Richardson et al., 2023].

The PB framework also served as a basis for the Doughnut economy framework, which extends the concept of *environmental ceiling* (i.e., ecological limits from the PB framework) with the concept of *social floor*. This aims at explicitly accounting for the *just* dimension associated with social aspects, on top of the *safe* dimension captured by the environmental aspects. In this work and in AESA in general, the *just* dimension is (partially) accounted for through the use of sharing principles when allocating the global carrying capacities. Yet, this relates more to distributive justice theory (i.e., sharing a limited resource) than social floor definition (i.e., meeting basic human needs/human satisfiers [Brand-Correa and Steinberger, 2017]).

2.2 Definition of the safe operating space

In practice, the PB framework provides boundaries that can be used as *global* carrying capacities at the Earth level. In fact, the PBs are limits at a global scale and they can be understood as the maximum quantities of various resources that could be used on Earth [Dao et al., 2018]. This directly refers to a key concept in the PB framework, i.e., the safe operation space (SOS), as depicted in Figure 1(a) with the green zone. It refers to the ability of the planet Earth to provide life support systems for humanity, i.e., the maximum value of the control variable that is allowed to reach before transgressing the planetary boundary [Vázquez et al., 2023]. The SOS is then often used in AESA studies to define global carrying capacities. There are two main approaches to define the safe operating space in the literature.

- **Approach #1 (Full SOS) :** The first approach removes the natural background level $CC_e^{NB}(t = \text{Holocene})$ from the planetary boundary value CC_e^{PB}, for each Earth system process e. The natural background level is the value of the control variable *before* human activities began affecting the Earth System process, i.e., the preindustrial Holocene base values [Richardson et al., 2023]. This approach is referred to as the *full* safe operating space available for humans [Ryberg et al., 2018]. In practice, this the most common approach in AESA studies [Ryberg et al., 2018,Stranddorf et al., 2023, Lejeune et al., 2026, Puig-Samper et al., 2025], and also the one used in the PB framework, as reported in Table 1. Nonetheless, it is important to point out that it defines *tangential (static) values* of the full SOS, or in other words the (maximal) situation that should be reached at the global level. The full SOS is therefore the space for human civilization to thrive without threatening the stability of the Earth system, i.e., while ensuring a "normal"/Holocene-like functioning of the Earth system. Equation 1 is inspired from [Lejeune et al., 2026] and defines the full SOS.

$$CC_e(t) = CC_e^{PB} - CC_e^{NB}(t)\big|_{t=Holocene} \tag{1}$$

- **Approach #2 (Remaining SOS):** On the contrary, the second approach removes the current value ($t = \text{today}$) of the control variable from the planetary boundary CC_e^{PB}, for each Earth system process e. This approach is referred to as the *remaining* safe operating space [Ryberg et al., 2018], as it captures the *currently* available SOS. However, authors in [Ryberg et al., 2018] argue that "it is not relevant for evaluating how an existing or planned activity can affect humanity's ability to maneuver within the total safe operating space. Instead, this approach is only relevant for showing if the introduction of a new activity will lead to exceedance of the PBs, assuming everything else remains the same". In fact, this approach leads to negative value SOS for Earth system processes where the current value of the control variable exceeds the boundary, which is the case of seven out of nine PB today [Sakschewski et al., 2025]. In practice, this approach is hence discouraged [Ryberg et al., 2018] because alternatives are found "not absolute environmentally sustainable" by-default, preserving the status quo through inaction, and therefore discouraging a potential improvement of the situation and a transition towards an environmentally sustainable society [Ryberg et al., 2018].

$$CC_e(t) = CC_e^{PB} - CC_e(t)\big|_{t=today} \tag{2}$$

2.3 Global static carrying capacities based on the planetary boundaries framework

This section details which planetary boundaries are considered in the UNCASExt framework (and implemented in `pyaesa`), together with each boundary values. Ideally, all planetary boundaries should be included in the SOS definition. However in practice, a subset of PBs can be selected when data are lacking or if the PB is clearly irrelevant to the study. In this study, eight out of nine Earth-system processes defined in the PB framework are considered. The planetary boundary for novel entities is excluded similarly to [Serrano et al., 2025, Vázquez et al., 2023], because there is no specific environmental threshold currently defined and because there is a lack of consensus concerning the adequate control variable [Persson et al., 2022]. Stratospheric ozone depletion and atmospheric aerosol loading Earth-system processes are both included although the coverage of environmental stressors available in multi-regional input-output (MRIO) databases is poor. This study therefore includes most of the PB that are currently exceeded at the global level [Sakschewski et al., 2025], similarly to [Serrano et al., 2025].

The full safe operating space from the PB framework is selected as the global carrying capacity (i.e., the finite resource) to be shared for each Earth system process, as detailed in Section 1. Values are taken directly from the scientific literature [Richardson et al., 2023, Sakschewski et al., 2025] and reported in Table 1. To ensure consistency in the ASR, both the numerator and the denominator must use consistent characterization factors [Bjørn et al., 2025]. The use of the PB framework for defining global carrying capacities hence requires the use of the PB-LCIA method [Ryberg et al., 2018] for the LCA (or conversely, the use of PB-LCIA for the LCA requires the use of the PB framework for defining carrying capacities). Characterization factors from [Ryberg et al., 2018] and [Yang and Paulillo, 2026] are therefore used. To maintain consistency with the PB-LCIA method used for the LCA (numerator of the ASR), control variables for freshwater use (blue water consumption) and biosphere integrity (functional diversity) are taken from the original version of the PB framework [Steffen et al., 2015], similarly to [Puig-Samper et al., 2025]. Characterization factors from [Galán-Martín et al., 2021] and [Vázquez et al., 2023][4] are used for biosphere integrity (functional diversity).

[4]See Appendix A in their supplementary material [Vázquez et al., 2023].

Table 1: Full safe operating space (SOS) definition based on the planetary boundary framework [Steffen et al., 2015, Sakschewski et al., 2025].

Earth system process	**Abbreviation**	**Control variable**	**Time dimension**	**DPSIR location**	**Unit**	**Planetary boundary (zone of uncertainty)**	**Natural background level**	**Current value (2025)** [Sakschewski et al., 2025]	**Full SOS (min)**	**Full SOS (max)**	**Ratio (max/min)**	**Sources**
Climate change (CO_2 concentration)	aCO2	Atmospheric CO_2 concentration	Implicit	State	ppm	350–450	278	423	70	170	2.43	Table 3 in [Sakschewski et al., 2025]
Climate change (energy imbalance)	EI	Total anthropogenic radiative forcing at top-of atmosphere	Implicit	State	W/m^2	1–1.5	0	2.97	1	1.5	1.5	Table 3 in [Sakschewski et al., 2025]
Ocean acidification	OA	Carbonate ion concentration, average global surface ocean saturation state with respect to aragonite (Ω_{arag})	Implicit	State	Ω_{arag}	2.5–2.86	3.57	2.84	0.82	0.71	0.87	Table 3 in [Sakschewski et al., 2025]
Stratospheric ozone depletion	SOD	Stratospheric O3 concentration (GLO average)	Implicit	State	DU	277–263	292	285.7	15	29	1.93	Table 3 in [Sakschewski et al., 2025]
Atmospheric aerosol loading	AAL	Interhemispheric difference in Aerosol Optical Depth (AOD)	Implicit	State	AOD	0.1–0.25	0.04	0.063	0.06	0.21	3.5	Table 3 in [Sakschewski et al., 2025]
Biogeochemical flows - N	N	Nitrogen GLO: industrial and intentional fixation of N	Explicit	Pressure	Tg N yr^{-1}	GLO: 62–82	0	165	62	82	1.32	Table 3 in [Sakschewski et al., 2025]
Biogeochemical flows - P	P	Phosphate GLO: P flow from freshwater systems into the ocean; regional: P flow from fertilizers to erodible soils	Explicit	Pressure	Tg P yr^{-1}	GLO: 11–100 REG: 6.2–11.2	0	GLO: 4.4 REG: 18.2	11 6.2	100 11.2	9.09 1.81	Table 3 in [Sakschewski et al., 2025]
Land-system change (GLO)	LSC	GLO: area of forested land as percentage of original forest cover; biome: area of forested land as percentage of potential forest	Implicit	State	%	GLO: 75–54%	100	GLO: 59%	25	46	1.84	Table 3 in [Sakschewski et al., 2025]
Freshwater use (GLO)	FWU	Blue water: human induced disturbance of blue water flow	Explicit	Pressure	km^3 yr^{-1}	GLO: 4000–6000	0	~2600 (2015)*	4000	6000	1.5	[Steffen et al., 2015]
Biosphere integrity (functional diversity)	BI FD	Functional diversity: Biodiversity Intactness Index (BII) loss	Explicit	Impact	% BII loss	10–70	0	16%(Southern Africa, 2015)*	10	70	7	[Steffen et al., 2015]; Lund et al, 2025
† Novel entities	NE	Percentage of synthetic chemicals released to the environment without adequate safety testing	Implicit	Pressure	/	0–NA	0	> 0	0	NA	NA	Table 3 in [Sakschewski et al., 2025]

GLO: Global. REG: Regional. †: Not included in this study. $\star$: Value from [Steffen et al., 2015] for 2015.

2.4 Difference between limits and targets

An important distinction between *limits* and *targets* should be pointed out. Based on Eurostat, authors of [Dao et al., 2018] define a target as "a value that the indicator should reach, accompanied or not by a deadline to achieve this value (target year)". It must therefore be clear that limits such as planetary boundaries are not targets because the goal is not to reach them. They rather act as an upper bound which should not be transgressed [Dao et al., 2018], given that unacceptable impacts are much more likely to occur. Nevertheless, returning to the limit may be set as a target for the PBs that have already being surpassed [Dao et al., 2018], as it is the currently the case for seven out of nine boundaries in the PB framework [Sakschewski et al., 2025]. The authors of [Lund et al., 2025] also argues that a planetary boundary should therefore not be understood as a global threshold or tipping point, because the planetary boundary is located upstream of the biophysical threshold and acts as a buffer for the tipping point of uncertain consequences of environmental impacts.

Boundary positions do not demarcate or predict singular threshold shifts in Earth system state: they are placed at a level where the available scientific evidence suggests that further perturbation of the individual process could potentially lead to systemic planetary change by altering and fundamentally reshaping the dynamics and spatiotemporal patterns of geosphere-biosphere interactions and their feedback. This strengthens the rationale for using the precautionary principle to set the planetary boundaries at the lower end of the zone of increasing risk [Richardson et al., 2023]. It is also important that these threshold values are determined by best available science, based on a large agreement from the scientific community, even if the uncertainty range is large [Dao et al., 2018]. They could then be used to inform political and business decision makers, and to set targets that will inherently depend on political will, perceptions of equity, efficiency and feasibility, among others. In fact, the authors of [Dao et al., 2018] highlight that targets are set through policy processes (often with short-term and achievable objectives in mind), and should be understood as the result of negotiations. This hence relates to dimensions such as power relations, economic considerations, public pressure, social values and perceptions. For instance, the limit can be seen as too difficult to attain, e.g. too expensive in economic terms [Dao et al., 2018]. This explains (at least partially) why a scientific limit (if identified) does not directly translate into an identical policy target [Dao et al., 2018].

2.5 Time dimension in the planetary boundaries framework

The authors of [Guinée et al., 2022] points out that planetary boundaries in the PB framework are related to a time dimension, which is often overlooked. In fact, they highlight that most (although not all) boundaries have a temporal dimension, being either *explicit* (e.g., rate of biodiversity loss in number of species per million per year, nitrogen cycle in millions of tonnes per year, phosphorous cycle in millions of tonnes per year, and global freshwater use in km^3 per year), or *implicit* (e.g., atmospheric CO_2 concentration is connected to annual CO_2 emissions, stratospheric ozone depletion is connected to CFC-emissions per year, etc). The time dimension for each Earth system process is further specified in Table 1.

It is important to remind the associated implications in the characterization of environmental flows, and especially in the PB-LCIA method, as explained by the authors of [Lund et al., 2025]. In fact, contrarily to conventional LCIA methods which encode life cycle information (LCI) information as mass, the PB-LCIA method give LCI information on resource use and emissions to the environment as *mass per year*. This hence allows for the results to be expressed directly in the metrics of the PB's control variables, i.e., as annual pressures or environmental states in a long-term (steady-state) perspective [Ryberg et al., 2018]. Consequently, if an anthropogenic activity is found to be absolute environmentally sustainable using the PB-LCIA method, the activity can be considered sustainable relative to the PBs *over an infinite time-horizon*, as explained in [Ryberg et al., 2018]. Yet, this also requires that the functional unit is defined over one year and assumes that it is to be perpetuated every year until the steady state

has been reached, as explained in [Guinée et al., 2022]. This has its implications for the interpretation, and it is often not stated explicitly by practitioners, or even misunderstood which can lead to erroneous interpretations of results. Considering temporal aspects in planetary boundaries and LCIA methods is important to ensure relevant interpretation of the results.

2.6 Uncertainty in carrying capacities definition

The full SOS definition in the PB framework embeds inherent uncertainty, as depicted in Table 1 through the lower and upper end of the zone of increasing risk. The authors in [Puig-Samper et al., 2025] model the full SOS as a left triangular probability distribution, where the mode is set to the minimal value of the zone of uncertainty and the maximal value to the higher end of it. This choice aims at representing the range of variation for carrying capacities while maintaining a preference for the precautionary approach, which is a normative choice aiming at maximizing the chance of respecting the Earth System [Puig-Samper et al., 2025, Steffen et al., 2015, Ryberg et al., 2018]. However, this complicates uncertainty discernibility and therefore interpretation, as the uncertainty contribution from the carrying capacities definition is mixed up with other uncertainties. In the UNCASExt framework, we therefore chose to use a min/max approach for the definition of the full SOS, rather than a left triangular probability distribution. This improves uncertainty discernibility in the final results, which hence improve results interpretation. The results are therefore always provided for the minimum value of the PB, and the ratio between the maximum and minimum value of the full SOS in provided in Table 1, which directly allows to transpose the results and the uncertainty distribution.

The underlying environmental process behind each boundaries definition could be discussed, but this is not the purpose of this work. In fact, this belongs to environmental sciences research field and it is simply assumed in this study that current planetary boundaries are the best currently available scientific estimates regarding control variable for keeping the Earth system in an Holocene-like state.

3 Global carrying capacities from other sources

There also exists other definitions of global carrying capacities, expressed with other control variables and in other units than the ones from the PB framework. Examples can be found in [Lund et al., 2025, Sala et al., 2020, Bjørn and Hauschild, 2015].

3.1 Global static carrying capacities adapted to the EF3.1 method

One of the most common alternative to the PB framework for defining global carrying capacities is the use the 16 midpoint indicators of the EF LCIA method, as provided by the Joint Research Center (JRC) [Sala et al., 2020]. An important difference with the carrying capacities defined in the PB framework is that the EF approach defines carrying capacities for several categories including human health or ecosystem health whereas planetary boundaries are only concerned with the stability and resilience of Earth system, i.e., not human or ecosystem health [Richardson et al., 2023]. Given that an increasing number of LCA and AESA studies are considering the EF method, global carrying capacities values for EF are also provided in Table 2. Note that updated values from the JRC [Sanye et al., 2023] are considered rather than the original ones from [Sala et al., 2020], which leads to (i) a decrease of about 0.3% for the eutrophication terrestrial category and the change of control variable for the land use category. Aside from these updates, the minimal carrying capacities defined in [Sanye et al., 2023] corresponds to the carrying capacities reported in [Sala et al., 2020]. For the GWP_100 LCIA method, the global static carrying capacity is the same as the one provided for climate change in Table 2. The UNCASExt framework supports carrying capacities from the PB framework and from the EF LCIA method (including GWP_100).

Table 2: Global carrying capacities adapted to the EF metrics of each impact category. Values taken from [Sanye et al., 2023].

EF impact category	**Abbreviation**	**Unit**	**CC** (min)	**CC** (max)	Ratio (max/min)	**Sources**
Climate change	GWP_100	kg CO2-eq	6.81×10^{12}	8.72×10^{12}	1.28*	[Sanye et al., 2023]
Ozone depletion	ODP	kg CFC-11-eq	5.39×10^{8}	1.08×10^{9}	2.00	[Sanye et al., 2023]
Particulate matter	PM	Disease incidence	5.16×10^{5}	1.03×10^{6}	2.00	[Sanye et al., 2023]
Ionising radiation	IR	kBq U-235-eq	5.27×10^{14}	1.05×10^{15}	1.99	[Sanye et al., 2023]
Photochemical ozone formation	POF	kg NMVOC-eq	4.07×10^{11}	8.13×10^{11}	2.00	[Sanye et al., 2023]
Acidification†	AC	mol H+ eq	1.00×10^{12}	2.00×10^{12}	2.00	[Sanye et al., 2023]
Eutrophication terrestrial	TEU	mol N-eq	6.11×10^{12}	1.22×10^{13}	2.00	[Sanye et al., 2023]
Eutrophication freshwater	FEU	kg P-eq	5.81×10^{9}	1.16×10^{10}	2.00	[Sanye et al., 2023]
Eutrophication marine	MEU	kg N-eq	2.01×10^{11}	4.01×10^{11}	2.00	[Sanye et al., 2023]
Ecotoxicity freshwater	ECOTOX	CTUe	1.31×10^{14}	2.63×10^{14}	2.01	[Sanye et al., 2023]
Human toxicity non-cancer	HTOX_nc	CTUh	4.10×10^{6}	8.20×10^{6}	2.00	[Sanye et al., 2023]
Human toxicity cancer	HTOX_c	CTUh	9.62×10^{5}	1.92×10^{6}	2.00	[Sanye et al., 2023]
Land use	LU	Pt	3.98×10^{15}	7.96×10^{15}	2.00	[Sanye et al., 2023]
Water use	WU	m3 water-eq	1.82×10^{14}	3.64×10^{14}	2.00	[Sanye et al., 2023]
Resource depletion fossils	FRD	MJ	2.24×10^{14}	4.48×10^{14}	2.00	[Sanye et al., 2023]
Resource depletion minerals and metals	MRD	kg Sb-eq	2.19×10^{8}	4.39×10^{8}	2.00	[Sanye et al., 2023]

†: The authors of [Sala et al., 2020] explains that the PB for ocean acidification was linked to climate change due to their strong cause-effect relationship. In fact, there was no link with the acidification impact category, as the underlying LCIA model only covers terrestrial acidification in the EF method.

*: As suggested in the supplementary material of [Sala et al., 2020], the uncertainty upper limit for climate change is set to 128% of the minimal SOS (as in [Steffen et al., 2015]) rather than 2× the PB for climate change.

3.2 Uncertainty in carrying capacities definition

The uncertainty in carrying capacity definition is handled similarly to what was introduced in Section 2.6 for the PB framework, i.e., with a min/max approach to ensure discernibility in final results. The uncertainty for minimal and maximal carrying capacity reported in Table 2 are directly taken from [Sanye et al., 2023]. Since a defined zone of uncertainty is not available for all the LCIA-based PBs, the authors of [Sala et al., 2020] arbitrarily set the fixed zone of uncertainty at two times (2×) the PB. To the best of authors' knowledge, no other approach was proposed since and the factor 2× is therefore also considered in UNCASExt. As suggested in the supplementary material of [Sala et al., 2020], the uncertainty upper limit for climate change is set to 128% of the minimal SOS (as in [Steffen et al., 2015]) rather than 2× the PB for climate change.

4 Alternative carrying capacities for climate change

4.1 Motivations

Alternative carrying capacities are defined for climate change in the literature, besides the two original ones from the PB framework, i.e., CO_2 concentration (aCO2) and energy imbalance (EI). One of the main motivation of defining alternative carrying capacities is to enhance the interpretation and the operationalization potential of the climate change boundaries at lower scales.

In practice, the key difference is that the control variable of these alternative carrying capacities is defined at a *pressure* level in the DPSIR impact pathway framework[5] rather than at a *state* level. This allows to move further up the causal chain of the environmental mechanisms leading to climate change [Dao et al., 2018] to focus on *pressure* rather than *state* variables (i.e., GHG annual emissions rather than energy imbalance or CO_2 concentration in the atmosphere), and hence include temporal aspects in the carrying capacity definition.

4.2 Main approaches in the literature

Several studies [Dao et al., 2018, Gebara and Laurent, 2023, Lejeune et al., 2026, Bjørn and Hauschild, 2015, Hadziosmanovic et al., 2022] have explored alternative PB definition for climate change based on climate targets as climate change is one of the planetary boundary that has received most attention up to now and hence, with more advanced modeling and analysis available. According to scientific literature, environmental boundaries for climate change can be obtained from carrying capacities mainly using (i) a **steady-state (static) approach** or (ii) a **budgeting (dynamic) approach**.

Both approaches are introduced below, but the key difference lies in the *time horizon definition*. In fact, the steady-state approach aims at estimating the annual emissions that would result (everything else being kept the same) in a steady-state condition corresponding to the level of the threshold value if these emissions were to be sustained indefinitely, whereas the budgeting approach defines the total emissions over a finite period of time (e.g., 100 years) that would result in the level of the threshold value. Eventually, the authors of [Gebara and Laurent, 2023] point out that both approaches are applicable to obtain thresholds for the climate change footprint indicator and that they should ideally be both included to reflect the variations between the two approaches and account for potential sensitivity in the thresholds.

Aside from the time dimension, the *risk* of moving away from the Holocene state, and the estimated relevancy of choosing one climate scenario or another (given or (in)ability as (parts of) human society to move towards this scenario) are two important considerations when defining an alternative carrying capacity for climate change. In fact, defining the climate change PB closer to a potential tipping point accepts a higher risk of moving away from Holocene state by choosing climate change scenarios that are relaxed compared to the original framework. Using value from the PB framework has the advantage to set the PB independently of the risk and difficulties to reach that target. The authors of [Dao et al., 2018] argue in their supplementary material that this value can be considered as a *theoretical reference* as no new evidences were found to contradict the fact that 350 ppm limit corresponds to a safe operating space [Hansen et al., 2013]. Authors of [Dao et al., 2018] also highlight in their supplementary material the fact that the original PB for climate change can be seen as very hard (or impossible) to reach in practice because of the tremendous transformations to be implemented in a very short time. This can

[5] To structure interactions between the environment and socioeconomic activities, the European Environment Agency (EEA) uses the driving force, pressure, state, impact, and response (DPSIR) framework. In practice, it is used for different means (e.g., design assessments, indicators identification, results communication, environmental monitoring improvement, information collection). Even though various conceptual frameworks exist for organizing drivers and pressures, the DPSIR framework has been widely accepted and commonly used in the global environmental change community [Jabbour and Hunsberger, 2014].

lead to "more realistic" SOS definition with higher associated risk levels. The second option is therefore a *pragmatic definition* of the SOS, although it is less ambitious and more influenced by the currently observed inability of (parts of) human civilizations to address climate change over the last decades. This may be seen as a form of path dependency in how environmental targets are defined and relaxed over time. Nevertheless, several studies [Lejeune et al., 2026, Lund et al., 2025, Gebara and Laurent, 2023, Dao et al., 2018] argue that SOS definition should be explicitly related to a climate target (i.e., a proxy of the risk level) to be meaningful.

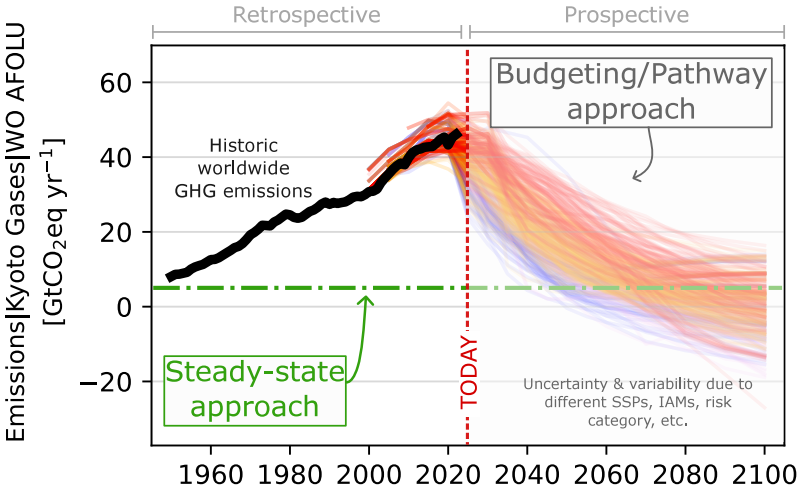

Figure 2: Static steady-state vs. dynamic carrying capacity definition for climate change (global). The static steady-state approach is illustrated with the annual budget of 6.81 $GtCO_2eq{\cdot}yr^{-1}$ associated to 2°C of global warming, according to [Bjørn and Hauschild, 2015] (assuming an infinite time period). The annual net GHG emissions (Kyoto gases, without AFOLU emissions) vary over time according to different IAMs, SSPs, and risk category (C1 to C4 corresponding to a global warming below 2°C by 2100) in the budgeting approach. Historic worldwide GHG emissions from PRIMAP-HIST data (v2.6.1) [Gütschow et al.,] are also shown via the solid black line. This illustrative figure mainly aims at highlighting the difference between a static and a dynamic approach.

4.2.1 Steady-state (static) approach

The steady-state approach consists in estimating the sustained level of *annual* emissions for each GHG (in $GtCO_2eq\ yr^{-1}$) which would result (everything else being kept the same) in a steady-state condition corresponding to the level of the threshold value, e.g., 2°C of global warming. However, few studies provide steady-state based thresholds for GHG emissions in the literature, as pointed out by [Gebara and Laurent, 2023]. One of the most referenced study is the one from [Bjørn and Hauschild, 2015], hence representing the primary source to derive carrying capacities for climate change. The authors of [Bjørn and Hauschild, 2015] report a value of 6.81 $GtCO_2eq\ yr^{-1}$ for 2°C of global warming. This explains for instance the value provided for climate change in Table 2. In the steady-state approach, there is therefore no start year or end year, as the time horizon is infinite. The authors of [Bjørn and Hauschild, 2015] also report a value of 3.61 $GtCO_2eq\ yr^{-1}$ associated with a radiative forcing of 1 W/m^2, which is seen as a more precautionary approach as it leads to a steady-state temperature increase of about 1.06°C above pre-industrial levels. This value was also used in [Gebara and Laurent, 2023]. However, no study has computed such a threshold for the control variable of 350 ppm of atmospheric CO_2. Although the steady-state approach is attractive as very simple, it also hides an important variability depending on the GHG considered which is not really explicit in the original paper of Bjørn and Hauschild [Bjørn and Hauschild, 2015].

4.2.2 Budgeting (dynamic) approach

The budgeting approach consists in estimating the remaining cumulative GHG emissions human activities can afford to emit before overshooting a target or exceeding a boundary [Gebara and Laurent, 2023]. The full SOS for climate change (pressure) can then be related to the total CO_2 emissions (or GHG emissions) over a period of time, i.e., a budget which can then be translated into annual emissions. This translation into annual emissions has the advantage to significantly improve operationalization, as it is easier for actors (countries, sectors, industries, companies, people, etc.) to evaluate the environmental performance of socio-economic activities at lower scales based on yearly emissions. The definition of the alternative carrying capacity for climate change with a budgeting approach is hence related to both (i) a time horizon for the emissions budget, and (ii) a level of risk that is judged *acceptable* (normative) regarding the consequences of global warming, i.e., a higher emissions budget will lead to an increasing global temperature.

This approach is by far more popular in the literature, as several studies have proposed emissions budgets in recent decades. Yet, [Gebara and Laurent, 2023] stress out that these budgets are based on different models and assumptions [Zhai et al., 2018, Rogelj et al., 2016], which clearly show discrepancies due to both physical uncertainties and value choices, e.g., incomplete understanding of the carbon cycle, choice of model type, historical emissions, target definition, budget definition, years of negative emissions, mitigation of non-CO_2 emissions in the chosen pathway, technology assumptions for carbon capture and sequestration (CCS), etc. Contrarily to the steady-state approach, the time horizon and the reference year must be specified with the budgeting approach.

Budgets estimation based on model-SSP-climate emissions pathways

The estimation of emissions budgets for climate change in the literature mostly rely on models (e.g., integrated assessment models (IAMs)), shared socioeconomic pathways (SSPs) [Riahi et al., 2017, Fricko et al., 2017], and climate pathways. This approach allows to explicitly relate carrying capacities definition to IAMs and SSPs [Lund et al., 2025, Lejeune et al., 2026, Clausen et al., 2025], as introduced in recent studies [Lund et al., 2025, Lejeune et al., 2026, Clausen et al., 2025]. The authors of [Lejeune et al., 2026] argued[6] that the allocation of an environmental space should be based on a future context leading to 1.9 W/m^2 by 2100. Their study further mentions that "allocating a share of the SOS using data from an SSP scenario of an IAM model not only provides a meaningful backbone since it ensures a possible path towards the operation of human activities within the SOS for climate change (...). Also, these SSP scenarios inherently tackle the social aspect as they maximise socio-economic welfare at regional levels to meet a climate target. However, no study comprehensively uses an SSP (SSP1-1.9) scenario to allocate a share of the SOS".

Annual emissions estimation

Most studies distribute GHG or CO_2 budgets over time such that decisions can be related to it in the context of operationalization and decision making, i.e., enabling the benchmarking of annual impacts. Annual emissions can therefore be extracted directly from IAMs, or by distributing the budget over time (e.g., equally across all remaining years, linearly, exponentially, etc) [Hadziosmanovic et al., 2022].

In the AESA literature, studies [Gebara and Laurent, 2023, Vázquez et al., 2023] also evaluate the annual average emissions that could be emitted for a year t, based on the total budget from a reference year

[6]The authors of [Lejeune et al., 2026] also mention that "no SSP combination will lead to human operation within the SOS by 2100. According to [Meinshausen et al., 2020], the closest matching combination is SSP1-1.9 with mitigation to 350 ppm CO_2 by 2150 and RF of approximately 1.5 W/m^2 (upper uncertainty zone of the radiative forcing boundary) by 2300".

to the time horizon (e.g., 2100) and the previous historical emissions. This is expressed mathematically by the authors of [Vázquez et al., 2023] as follows:

$$CC_e(t) = \begin{cases} \frac{CC_e^{c_{t_0,t_f}}}{2100-t_0} & t = t_0 \\ \frac{CC_e^{c_{t_0,t_f}} - \sum_{t=t_0}^{t=t-1} CV_{e,t}}{2100-t} & \forall t \in \{t_0+1, ..., t_f\} \end{cases} \quad (3)$$

where $CC_e^{c_{t_0,t_f}}$ is the total emissions budget from t_0 (reference year) until $t_f = 2100$, and $CV_{e,t}$ the control variable for emissions at a given year t.

This can also be applied to obtain an average constant value for emissions until $t_f = 2100$. For instance, the authors of [Gebara and Laurent, 2023] benchmarked values from [Robiou du Pont et al., 2017] against annual impacts by distributing the budgets equally over the assessed period (i.e. 83 years), after correcting for historical emissions from 2010 to 2018. The authors in [Gebara and Laurent, 2023] motivate the choice of the time horizon for climate change (i.e., 2100) by existing models, scenarios, and pathways suggesting possibilities to bring current levels of impacts below thresholds. They obtained the final thresholds for the 2°C of 16.6 $GtCO_2eq/yr$ (min-max: 10.7-26.9 $GtCO_2eq$) and for the 1.5°C of 9.5 $GtCO_2eq/yr$ (min-max: 1.4-17.1 $GtCO_2eq$). The authors in [Gebara and Laurent, 2023] also relied on IAM models, although they pointed out that no emission budget was currently available in the literature to align with the planetary boundaries from the PB framework [Rockström et al., 2009b, Steffen et al., 2015]. They hence applied the open source MAGICC[7] climate model [Meinshausen et al., 2011] to form scenarios consistent with reaching a radiative forcing of 1 W/m^2 and an atmospheric CO_2 concentration of 350 ppm CO_2 in 2100. The resulting mean budget estimates were found to be -60 $GtCO_2eq$ (min-max: -139-17 $GtCO_2eq$) and 484 $GtCO_2eq$ (min-max: 431-556 $GtCO_2eq$) for 1 W/m^2 and 350 ppm CO_2, respectively. This led to corresponding annual *average* thresholds used in their assessment (for the reference year 2018) equal to -0.72 and 5.8 $GtCO_2eq/yr$ for the PBs of 1 W/m^2 and 350 ppm CO_2, respectively. It is important to highlight that "the cumulative budget over the full period should therefore be considered as the original threshold, whilst the annual mean value seeks to express the budget on an annual basis" [Gebara and Laurent, 2023].

However, we argue that the annual average approach for distributing budgets over time has (at least) two main limitations. First, it is unrealistic and difficult to interpret because it does not consider transition from current state to a potential future and because constant average emissions is not capturing socio-technico-economic system's dynamics. Then, it is only valid from a budget-to-2100 point of view if historical emissions get back to the annual average at some point and stick to it afterwards. Consequently, the next sections introduce the systematic approach proposed in this work for defining alternative carrying capacities for climate change in the context of AESA studies.

[7] http://www.magicc.org/

4.3 Systematic definition of alternative dynamic carrying capacities for climate change

This section details the general systematic approach used in this work to define *global dynamic* carrying capacity for climate change, i.e., GHG and CO_2 emissions. This extends the approach proposed in recent studies [Lund et al., 2025,Lejeune et al., 2026] and proposes a systematic way to further include SSP scenarios in AESA studies, as an explicit parameter. Budgets are estimated based on IAM-SSP-climate pathways data from the International Institute for Applied Systems Analysis (IIASA) database [Byers et al., 2022] and historic data over the period $(t_{hist,0} - t_{hist,f})$ are used to harmonize emissions in the harmonization year $t_h = t_{s,0}$. This allows to provide budgets for any specific study period $(t_{s,0} - t_{s,f})$ of interest (with $2000 < t_{s,0} < t_{hist,f}$ and $t_{s,f} \leq 2100$, $t_{s,0} < t_{s,f}$), which ensures flexibility for a wide range of AESA studies. A high-level overview of the systematic approach is depicted in Figure 3, and each step is further detailed in the following sections. This systematic approach is implemented in the `pyaesa` Python package supporting the UNCASExt framework.

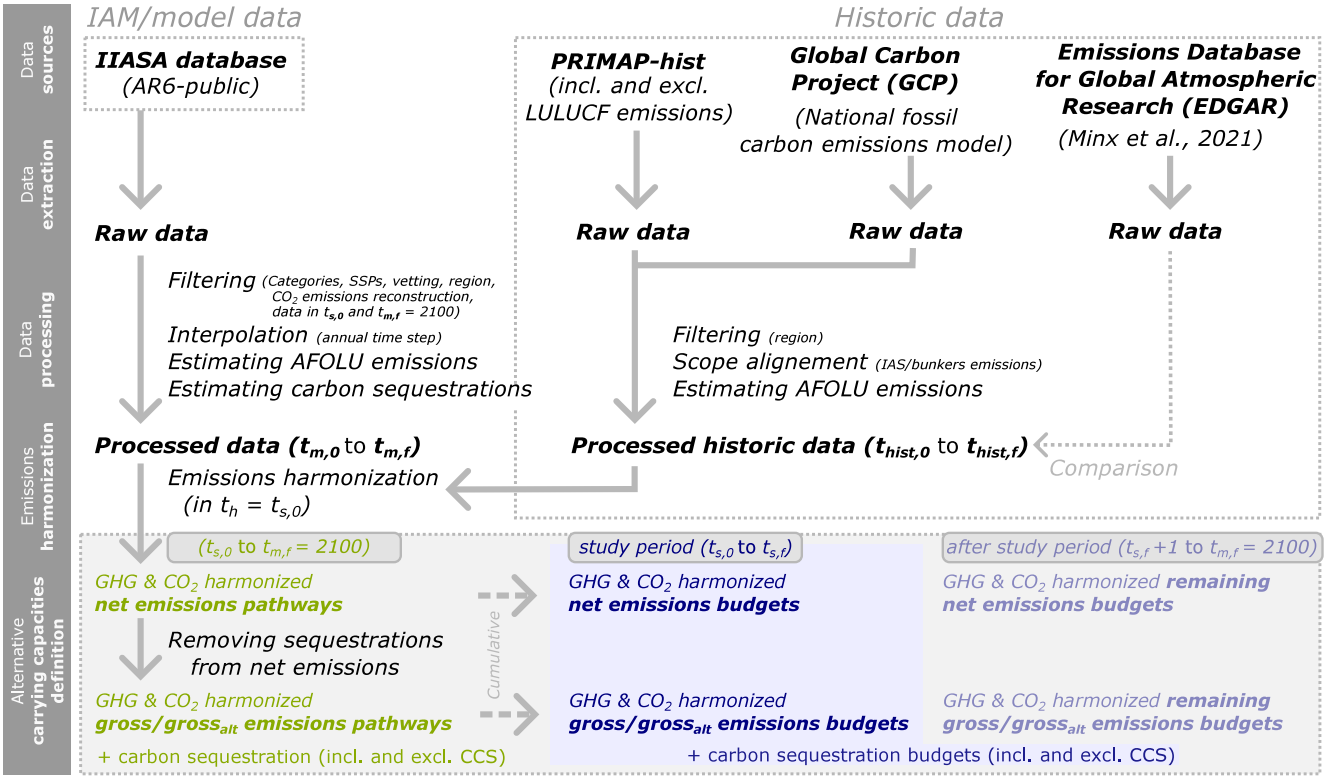

Figure 3: Systematic approach to define alternative climate change carrying capacities for a study period $(t_{s,0} - t_{s,f})$ of interest.

When defining the carrying capacity for climate change, a decision must be made regarding whether or not Land Use, Land-Use Change, and Forestry (LULUCF) emissions must be part of the emissions to be shared. In fact, the authors of [Robiou du Pont et al., 2017] argue that "emissions of the LULUCF sector are not considered by all parties as part of the emissions scope to be negotiated. Moreover, no universal accounting method of positive or negative LULUCF emissions is currently in place. This therefore supports the exclusion of LULUCF emissions from the global scenarios before allocating their emissions across countries". In practice, LULUCF emissions are a subset[8] of AFOLU emissions, which could therefore extend the concern to AFOLU emissions. To ensure flexibility and consistency in the

[8]LULUCF emissions can be a significant subset of AFOLU emissions. In fact, Figure 7.3 in the IPCC AR6 report (WGIII, Chapter 7) shows that LULUCF (CO_2) emissions represent more than 50% of the annual AFOLU (GHG) emissions.

definition of the carrying capacity, both options are implemented in this work, i.e., carrying capacity *including* and *excluding* AFOLU emissions.

In the following sections, GHG emissions are understood as Kyoto Gases emissions. The decision of focusing on GHG emissions rather than CO_2 emissions is motivated by the aim to capture more entities than CO_2, as this is the case in LCA for the climate change impact category. Nevertheless, including non-CO_2 emissions in emissions budgets is also criticized in the literature [Hadziosmanovic et al., 2022], since this involves several temporal and physical uncertainties[9]. Yet, the authors in [Hadziosmanovic et al., 2022] point out that it is important that future research explores more scientifically robust approaches to guide non-CO_2 mitigation. To ensure flexibility and consistency in the definition of the carrying capacity, both options are implemented in this work as illustrated in Figure 3, i.e., carrying capacity definition for GHG emissions and CO_2 emissions. It is important to remind that the carrying capacity is the budget over the study period, not the yearly emissions [Gebara and Laurent, 2023]. The temporal horizon 2100 is usually chosen as it is a long-term time horizon used in most climate models. The 2100 horizon is therefore also chosen in this study.

4.3.1 Estimation of historical emissions (GHG and CO_2 emissions)

4.3.1.1 Data extraction

Historic data are extracted from two sources, namely PRIMAP-hist[10] v2.7 [Gütschow et al., 2025] and the Global Carbon Project (GCP) [Friedlingstein et al., 2024]. This choice is mainly supported by their use in the context of the AR6, which reinforce internal consistency. A third source is considered for historical emissions in order to have an external comparison. This relies on the historical data file from the IIASA AR6 database, which is based on EDGAR data from [Minx et al., 2021], 2021 update of their dataset (v4)[11].

PRIMAP-hist data are provided both including and excluding LULUCF contributions[12], which is useful to estimate AFOLU emissions, as detailed in the following section. However, PRIMAP-hist data do not include emissions from international aviation and shipping (IAS). These emissions are therefore taken from the Global Carbon Project (GCP) data, more specifically from their national fossil carbon emissions modeling (territorial emissions). Emissions from IAS are assumed to be best represented by *bunkers emissions* in GCP, as they capture emissions from both international aviation and maritime transport. As GCP only report CO_2 emissions (no GHG emissions) for IAS emissions, IAS emissions may be underestimated for GHG emissions.

[9] The authors in [Hadziosmanovic et al., 2022] mention for instance variations in scenarios regarding the assumptions made about future non-CO_2 mitigation strategies, and additional uncertainties related to the radiative forcing and response of non-CO_2 emissions (e.g., short-lived climate pollutants like methane do not accumulate in the climate system in the same way in which CO_2 emissions do.

[10] As detailed on the PRIMAP-hist documentation [Gütschow et al., 2025], "The PRIMAP-hist dataset combines several published datasets to create a comprehensive set of greenhouse gas emission pathways for every country and Kyoto gas, covering the years 1750 to 2024, and almost all UNFCCC (United Nations Framework Convention on Climate Change) member states as well as most non-UNFCCC territories. The data resolves the main IPCC (Intergovernmental Panel on Climate Change) 2006 categories".

[11] Note that a newer version is now available (v6) thanks to an update in 2022 [Minx et al., 2022].

[12] As detailed by PRIMAP-hist documentation [Gütschow et al., 2025], "Version 2.7 of the PRIMAP-hist dataset does not include emissions from Land Use, Land-Use Change, and Forestry (LULUCF) in the main file. LULUCF data are included in the file with increased number of significant digits and have to be used with care as they are constructed from different sources using different methodologies and are not harmonized. (...) Emissions from Land Use, Land-Use Change, and Forestry (LULUCF) are included in the version without rounding as users need to take extra care when using LULUCF data because changes some of the year-to-year changes in the data come from using different sources or methodology changes within a source rather than changes in actual emissions."

For PRIMAP-hist data, the AR6GWP100 variable was used for GHG emissions (Kyoto Gases) and the HISTTP scenario was selected[13], i.e., third-party data are prioritized over country-reported data.

4.3.1.2 Data processing

Given that only *global* carrying capacities are to be defined in the UNCASExt framework, only emissions reported at the World level are considered for historical emissions (no distinction at the national level).

While PRIMAP-hist start reporting historical emissions in 1750, GCP provides data since 1850. Given that GCP data are only used for bunkers emissions and given that these emissions are reported to be zero before 1950, the start year of historic data $t_{h,0}$ can be set to the one from PRIMAP-hist (i.e., 1750). However, the end year of historic data $t_{h,f}$ is set to the last year of GCP data (2023) to ensure that the scope of each historic data point is consistent. After this processing step, historic data used in this study therefore encompasses IAS emissions.

Finally, AFOLU contributions in historic data are estimated based on the PRIMAP-hist definitions of AFOLU emissions. As detailed in PRIMAP-hist documentation [Gütschow et al., 2025], "*PRIMAP-hist uses a distinction between agriculture and Land Use, Land Use Change and Forestry which are combined into the AFOLU sector in IPCC2006 categories. Thus, in contrast to the standard IPCC 2006 categories, category 3 "Agriculture, Forestry, and Other Land Use" is subdivided as follows:*"

- (3) Agriculture, Forestry, and Other Land Use (**AFOLU**)[14]
  - (M.AG) AG Agriculture
    - (3.A) Livestock
    - (M.AG.ELV) Agriculture excluding Livestock
- (M.LULUCF) Land Use, Land Use Change, and Forestry

In the general organization of PRIMAP-hist data [Gütschow et al., 2025], this is summarized by:

- (0) National Total
  - (M.0.EL) Total emissions excluding LULUCF
    - (1) Energy
    - (2) Industrial Processes and Product Use
    - (4) Waste
    - (5) Other
    - (M.AG)
  - (M.LULUCF) Land Use, Land Use Change, and Forestry

Given that PRIMAP-hist comes by default excluding LULUCF emissions, M.AG emissions should be substracted from M.0.EL emissions to obtain historical emissions excluding AFOLU. On the contrary, historical emissions including AFOLU are obtain simply by adding LULUCF emissions, as M.AG emissions are already accounted for in M.0.EL emissions. Adopting the nomenclature commonly used in the integrated assessment modeling community, the estimation of historical emissions can therefore be expressed as follows:

[13] Choosing the HISTCR scenario (i.e., country-reported data are prioritized over third-party data) would lead to a decrease of total cumulative emissions (1750-2023) ranging from less than 1% up to 6%.

[14] PRIMAP-hist data for LULUCF emissions and Agriculture emissions is limited to three gazes, i.e., CO_2, CH_4, N_2O. National total (M.0.EL) emissions are however also accounting for F-gazes, in line with the list of Kyoto gases.

Table 3: Historical variables.

Variable	Expression
Emissions|CO2	Emissions|CO2|M.0.EL + Emissions|CO2|M.LULUCF + Emissions|CO2|Bunkers
Emissions|CO2|WO AFOLU	Emissions|CO2|M.0.EL - Emissions|CO2|M.AG + Emissions|CO2|Bunkers
Emissions|Kyoto Gases	Emissions|Kyoto Gases|M.0.EL + Emissions|Kyoto Gases|M.LULUCF + Emissions|CO2|Bunkers
Emissions|Kyoto Gases|WO AFOLU	Emissions|Kyoto Gases|M.0.EL - Emissions|Kyoto Gases|M.AG + Emissions|CO2|Bunkers

The resulting historical emissions for GHG and CO_2 emissions are depicted in Figure 4, which provides important observations. First, it appears clearly that LULUCF emissions from PRIMAP-hist embeds a sudden drop of Kyoto gases LULUCF emissions around 1990, both in the case of GHG emissions and CO_2 emissions. Then, emissions from bunkers (IAS emissions) account for up to 2.4% (2.8%) of total GHG emissions (incl. and excl. AFOLU emissions, respectively) and up to 3.2% (3.3%) of total CO_2 emissions (incl. and excl. AFOLU emissions, respectively). In addition, Figure 4 shows that agriculture emissions are mostly made of other GHG than CO_2, i.e., CH_4 and N_2O. Finally, the comparison with the EDGAR data (including AFOLU) suggests that GHG emissions (including AFOLU) in PRIMAP-hist may be underestimated, or at least belong to the lower range of EDGAR data for GHG and CO_2 emissions [Minx et al., 2021].

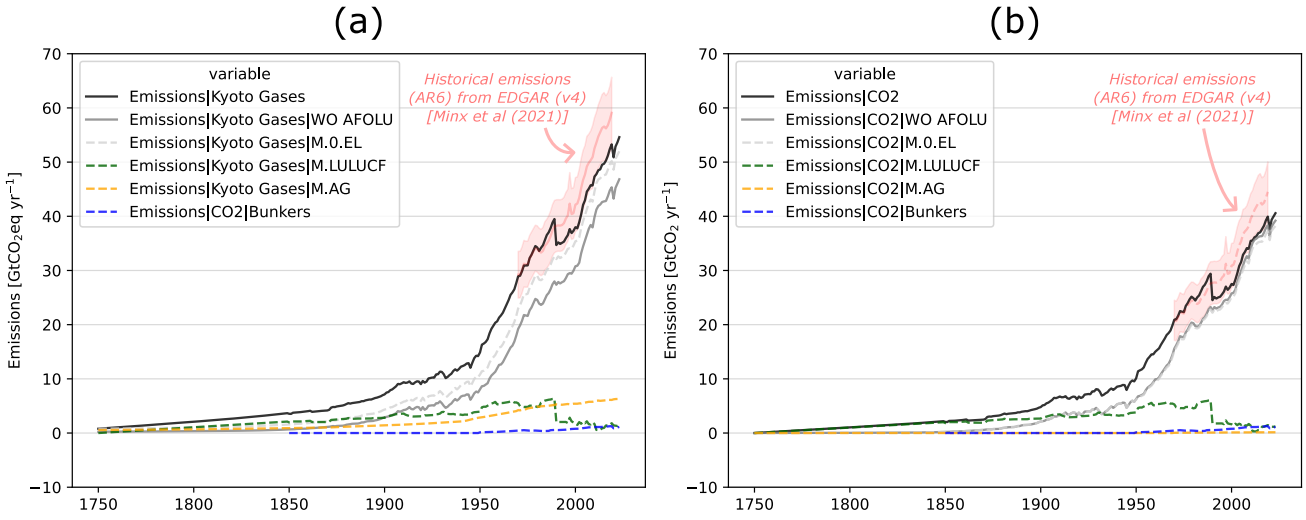

Figure 4: Historical (a) GHG emissions and (b) CO_2 emissions based on data from PRIMAP-hist and Global Carbon Project (for IAS emissions). The red-shaded area represents the range of historical emissions reported in [Minx et al., 2021] (EDGAR data, v4), with the solid red line being the reference values in the dataset.

4.3.2 Estimation of (harmonized) GHG and CO_2 budgets and annual emissions

4.3.2.1 Data extraction

The IIASA Energy, Climate, and Environment Program hosts a suite of Scenario Explorer instances and related database infrastructure[15] to support analysis of integrated-assessment pathways in Intergovernmental Panel on Climate Change (IPCC) reports and model comparison projects. In particular, the AR6 Scenario Explorer [Byers et al., 2022] (AR6-public) hosted by IIASA was selected in this work as it is the most update SE (2022) and because it presents an ensemble of quantitative, model-based pathways underpinning the Sixth Assessment Report (AR6) of Working Group III by the IPCC. GHG and CO_2 emissions pathways are directly extracted from the IIASA database [Byers et al., 2022].

4.3.2.2 Data processing

Filtering

Given that only *global* carrying capacities are to be defined, only data relevant at the World level are considered (no distinction at the national level).

Among close to 1800 variables available in the AR6 Scenario Explorer, a subset of 17 variables were selected, as listed in Table 4. These variables are sufficient in the context of this work, in addition to more than twenty metadata categories. For emissions variables (i.e., `Emissions|...`), several options are available in the AR6 database. This includes native emissions variables as the ones reported in Table 4, but also infilled[16] emissions variables (i.e., `AR6 climate diagnostics|Infilled|Emissions|...` and `AR6 climate diagnostics|Native-with-Infilled|Emissions|...`). However, even though infilled emissions in the AR6 database aim at comprising a more complete basket of GHGs, they are not available for all models (leading to incorrect values), and it is unclear if the variables for sub-contributions of AFOLU emissions are also infilled. Consequently, non-infilled emissions variables are considered in this work, as reported in Table 4.

Within the AR6 SE, hundreds of models and scenarios can be selected, all providing different pathways and capturing different modelling assumptions. More than 100 models are available[17] in the AR6 Scenario Explorer. All models-scenarios defined for the World region are considered to capture inter-model variability in the estimation of GHG and CO_2 emissions budgets. This results in more than 2300 scenarios gathered in the AR6 Scenario Explorer, as one model often provide several scenarios.

[15] In addition to support directly high-profile use cases such as the IPCC' Sixth Assessment Report (AR6) and the Horizon 2020 project ENGAGE [IIASA, 2025a], IIASA's modeling platform infrastructure allows the underlying datasets to be queried directly via a Rest API with the pyam package [IIASA, 2025b]. This creates a very effective environmental to pull data in a Python workflow.

[16] The infilling step is described in [Kikstra et al., 2022] as the inference of representative trajectories from the wider literature to close data gaps in emissions scenarios (such as time evolutions for some individual gas or aerosol species that are not reported by a given IAM) for missing species. Although there is no unique way to infill scenarios with missing data [Kikstra et al., 2022], this is often done based on a set of heuristics to infill missing F-gas, carbonaceous aerosols, synthetic estimates of black and organic carbon, and/or nitrate emissions, among others [Kikstra et al., 2022].

[17] This includes for instance POLES ENGAGE, AIM/CGE 2.0-2.1-2.2, POLES CD-LINKS, WITCH5.0, MESSAGEix-GLOBIOM 1.0-1.1, REMIND-MAgPIE, IMAGE, among others. 110 models are available in the "AR6_Scenarios_Database_World_v1.1.csv" file while about 189 models are available from the server at the time of writing. Nevertheless, considering only World as the target region provides the same list.

Table 4: Subset of included variables from the IIASA AR6 scenario explorer.

Variable	Unit	Description (IIASA AR6 SE)
Emissions|CO2	$MtCO_2\ yr^{-1}$	Total net-CO_2 emissions from all sources
Emissions|CO2|Energy	$MtCO_2\ yr^{-1}$	CO_2 emissions from energy use on supply and demand side (IPCC category 1A, 1B)
Emissions|CO2|Industrial Processes	$MtCO_2\ yr^{-1}$	CO_2 emissions from industrial processes (IPCC categories 2A, B, C, E)
Emissions|CO2|Energy and Industrial Processes	$MtCO_2\ yr^{-1}$	CO_2 emissions from energy use on supply and demand side (IPCC category 1A, 1B) and from industrial processes (IPCC categories 2A, B, C, E)
Emissions|CO2|Waste	$MtCO_2\ yr^{-1}$	No description
Emissions|CO2|Other	$MtCO_2\ yr^{-1}$	CO_2 emissions from other sources
Emissions|CO2|AFOLU	$MtCO_2\ yr^{-1}$	CO_2 emissions from agriculture, forestry and other land use (IPCC category 3)
Emissions|CO2|AFOLU|Land	$MtCO_2\ yr^{-1}$	CO2|AFOL emissions from forestry and other land use
Emissions|CH4|AFOLU	$MtCH_4\ yr^{-1}$	CH_4 emissions from agriculture, forestry and other land use (IPCC category 3)
Emissions|N2O|AFOLU	$ktN_2O\ yr^{-1}$	N_2O emissions from agriculture, forestry and other land use (IPCC category 3)
Emissions|Kyoto Gases	$MtCO_2eq\ yr^{-1}$	No description
Carbon Sequestration|CCS	$MtCO_2\ yr^{-1}$	Total carbon dioxide emissions captured and stored in geological deposits (e.g. in depleted oil and gas fields, unmined coal seams, saline aquifers) and the deep ocean.
Carbon Sequestration|Direct Air Capture	$MtCO_2\ yr^{-1}$	Total carbon dioxide sequestered through direct air capture
Carbon Sequestration|Enhanced Weathering	$MtCO_2\ yr^{-1}$	Total carbon dioxide sequestered through enhanced weathering
Carbon Sequestration|Feedstocks	$MtCO_2\ yr^{-1}$	Total carbon dioxide sequestered in feedstocks (e.g., lubricants, asphalt, plastics)
Carbon Sequestration|Land Use	$MtCO_2\ yr^{-1}$	Total carbon dioxide sequestered through land-based sinks (e.g., afforestation, soil carbon enhancement, biochar)
Carbon Sequestration|Other	$MtCO_2\ yr^{-1}$	Total carbon dioxide sequestered through other techniques

According to AR6 documentation, stored amounts should be reported as positive numbers for carbon sequestration.
Note that Emissions|CO2 and Emissions|Kyoto Gases variables are renamed to Emissions(net)|CO2 and Emissions(net)|Kyoto Gases in `pyaesa` for the sake of clarity.

Among all available models and scenarios, only a subset of scenarios are considered while others are filtered out. The conditions[18] for a scenario to be considered in the UNCASExt framework are threefold:

1. being explicitly associated to a **category** ranging from C1 to C4 (see Table 5) *and*,
2. being associated to a **shared socio-economic pathway** (SSP) [Riahi et al., 2017, Fricko et al., 2017] family (SPP1 to SSP5), *and*
3. being a **vetted** scenario (vetting "pass") in the IIASA AR6 database, i.e., complying with reporting standards and being within ranges of uncertainty [Kikstra et al., 2022].

This specific filtering is motivated by three reasons. The first reason is that we want the definition of the carrying capacity to be explicitly related to a level of *risk*, associated with the average warming of surface temperature by 2100, which is captured by the *category*[19] and illustrated in the Figure 6. The main goal is to directly support policy-making in the definition of the global carrying capacity by choosing a level of risk that is aligned either with an ambitious understanding of the Paris Agreement (PA) objectives (1.5°C of global warming in 2100) or with a more relaxed understanding of the PA objectives (2°C of global warming in 2100).

The second reason is that each scenario must be clearly classified in an SSP family to ensure a match of the SSP scenario between numerator and denominator of the ASR during the Monte Carlo simulations. In practice, if *premise* is used for generating results for the numerator, only a subset of SSP family could be used as *premise* only covers SSP1, SSP2, SSP3 and SSP5. Morevoer, only SSP1 to SSP3 are associated with a maximum of 2°C of global warming in *premise*, hence limiting the scope to SSP1 to SSP3.

The third reason is that to ensure consistency of scenarios, only vetted scenarios are included.

Some additional filters are applied to ensure that budgets estimation could be carried out properly. Scenarios must for instance provide data such that $t_{m,0} \leq t_{s,0}$ and $t_{m,f} = 2100$ (to ensure that all remaining budgets computed for $t > t_{s,f}$ rely on models-scenarios defined until the same time horizon), and

[18] Note that this filtering can be modified by the user if it is needed to cover a wider range of categories, or to include non-vetted scenarios for instance.

[19] *C1*: limit warming to 1.5°C (>50%) with no or limited overshoot, *C2*: return warming to 1.5C (>50%) after a high overshoot', *C3*: limit warming to 2°C (>67%), *C4*: limit warming to 2°C (>50%), *C5*: limit warming to 2.5C (>50%), *C6*: limit warming to 3C (>50%), *C7*: limit warming to 4°C (>50%).

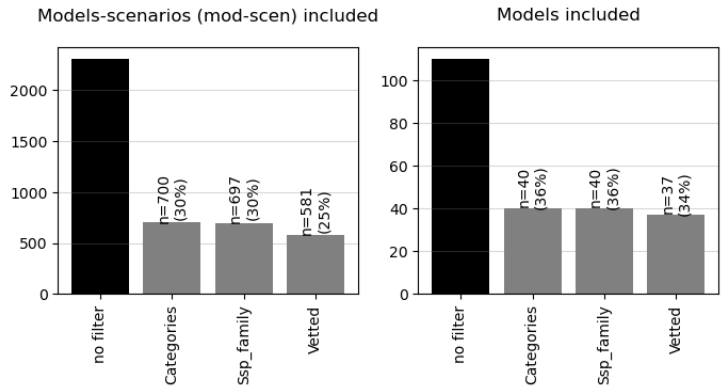

Figure 5: Effect of filtering all models-scenarios available in the AR6-public database according to (i) categories, (ii) SSPs, and (iii) vetted scenarios. The bar plot for each filter shows the resulting combination of current and previous filters, i.e., the last bar plot shows the combinations of the three filters.

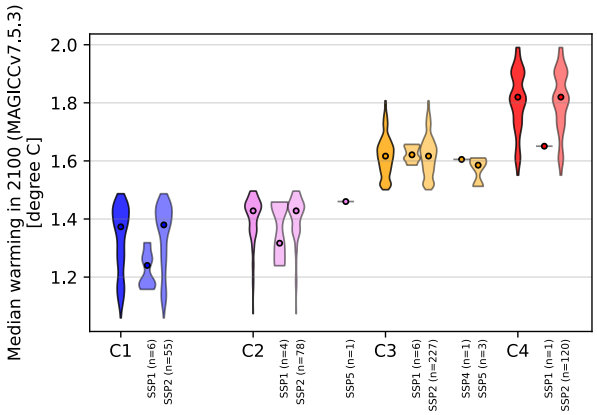

Figure 6: Median warming in 2100 (according to MAGICCv7.5.3) for all models-scenarios available after the filtering process on the AR6-public database. Models-scenarios are sorted by category and SSP, which clearly shows the increasing temperature in 2100 for higher categories.

provide data for the AFOLU selected variables (to allow the estimation of AFOLU emissions). An other filtering step is that only scenarios for which the variable 'Emissions|CO2' can be reconstructed from its sub-contributions (see in Table 4) with an error below an arbitrary threshold chosen to be 0.001% (of total cumulative CO_2 emissions over the whole the model period) are considered. In practice, this filter out about 10% of pre-filtered models-scenarios. For a study period 2019-2060, the filtering process ultimately yields a total of 494 scenarios considered, i.e., about 21% of all available scenarios in the IIASA AR6-public database. The number of scenarios drop from 581 to 524 with the extra-filtering steps while the numbers of models considered drop from 37 to 27. As illustrated in Figure 5, the filtering on 'Categories' is responsible for the most significant decrease of included scenarios, i.e., about 70% of the AR6 explorer scenarios are filtered out.

Table 5: Temperature classification rules used in AR6 WGIII. A scenario is placed in the lowest category where it meets the classification rule [Kikstra et al., 2022].

Category	Description	Classification rules
C1	Limit warming to 1.5°C (>50%) with no or limited overshoot	<1.5°C peak warming with ≥33% chance and <1.5°C end of century warming with >50% chance
C2	return warming to 1.5°C (>50%) after a high overshoot	<1.5°C peak warming with <33% chance and <1.5°C end of century warming with >50% chance
C3	Limit warming to 2°C (>67%)	<2°C peak warming with >67% chance
C4	Limit warming to 2°C (>50%)	<2°C peak warming with >50% chance
C5	Limit warming to 2.5°C (>50%)	<2.5°C peak warming with >50% chance
C6	Limit warming to 3°C (>50%)	<3°C peak warming with >50% chance
C7	Limit warming to 4°C (>50%)	<4°C peak warming with >50% chance
C8	Exceed 4°C warming (≥50%)	≥4°C peak warming with ≥50% chance

Interpolation

For all included scenarios, an interpolation of emissions is needed on the AR6 Scenario Explorer given that most scenarios provide data every 5 (or 10) years. Linear interpolation is hence carried out with an annual time step to provide annual emissions from the model base year $t_{m,0}$ to the model time horizon $t_{m,f}$, i.e., 2100.

Scope alignment

Emissions from IAS are assumed to be included as variables exist in the AR6-public database for aviation (e.g., capacity, energy, CO_2, etc), hence suggesting at least the inclusion of aviation.

AFOLU emissions

The AR6 Scenario Explorer does not provide explicit variables for GHG emissions emissions excluding AFOLU emissions. Nevertheless, variables are provided for GHG emissions emissions (including AFOLU emissions) together with variables for AFOLU emissions for CO_2, CH_4, N_2O. AFOLU emissions in the AR6 IIASA database [Byers et al., 2022] are reported in the documentation as "emissions from agriculture, forestry and other land use (IPCC category 3)". This therefore suggests[20] that AFOLU emissions (covering agriculture, forestry and other land use) are included by default in Emissions|Kyoto Gases and Emissions|CO2. The contributions of LULUCF emissions in AFOLU emissions are captured in the variables Emissions|CO2|AFOLU|Land, Emissions|CH4|AFOLU|Land, and Emissions|N2O|AFOLU|Land. GHG emissions excluding AFOLU emissions are therefore estimated in this work by removing AFOLU emissions of these three GHG. AR6 characterization factors (AR6 WG I, Chapter 7; Section 7.6.1.1) are used to obtain emissions in CO_2eq, as the emissions of these three gases are provided in native emissions for each gas. Specifically, CF_{CO2} = 1 $MtCO_2eq/MtCO_2$, CF_{CH4} = 27 $MtCO_2eq/MtCH_4$, and CF_{N2O} = 278 $MtCO_2eq/MtN_2O$. CO_2 emissions excluding AFOLU emissions are obtained by simply removing the Emissions|CO2|AFOLU emissions, as detailed in Table 6. This is applied independently for each model-scenario.

[20] More explicit documentation could not be found, to the best of our knowledge.

Table 6: Variables including and excluding AFOLU.

Variable	Expression
Emissions|CO2|WO AFOLU	Emissions|CO2 - Emissions|CO2|AFOLU
Emissions|Kyoto Gases|AFOLU	CF_{CO2} × Emissions|CO2|AFOLU + CF_{CH4} × Emissions|CH4|AFOLU + CF_{N2O} × Emissions|N2O|AFOLU
Emissions|Kyoto Gases|WO AFOLU	Emissions|Kyoto Gases - Emissions|Kyoto Gases|AFOLU

Note that Emissions|CO2|WO AFOLU, and Emissions|Kyoto Gases|WO AFOLU variables are renamed to Emissions(net)|CO2|WO AFOLU, and Emissions(net)|Kyoto Gases|WO AFOLU in `pyaesa` for the sake of clarity.

4.3.2.3 Emissions harmonization

In practice, it is very unlikely that the first year of the study period $t_{s,0}$ always fits with the model base year $t_{m,0}$. Not accounting for this difference in the start year can introduce a distortion on the total cumulative emissions, which will therefore not be consistent with the original features and properties of the scenario. Moreover, considering several scenarios from different models brings additional complexity to this challenge, as models-scenarios often start in a different different base year $t_{m,0}$. Nevertheless, this situation is not new in the integrated assessment modeling community given that new IAM keep on being developed (with different $t_{m,0}$) while requiring comparison to older IAMs. This can be done through **emissions harmonization** [Gidden et al., 2018], which refers to the process used to match emissions results from IAMs against a common source of historical emissions (GHG, CO_2, etc). As explained in [Gidden et al., 2018], the main goals of emissions harmonization are (i) to align model results in the harmonization year to a common historical data source, (ii) to faithfully represent the original IAMs internal consistency between the driver of emissions and emissions, and (iii) to maintain critical parameters from the original scenario design. In other words, this hence ensures that resulting future trajectories are consistent with the original modeled results while providing a *smooth* transition from the common historical data. Harmonization is a common exercise in the IAM community and this can be carried out with different methods and with different levels of granularity, e.g., accounting for sectoral dimensions, accounting for several emissions species, etc. The authors in [Gidden et al., 2018] have proposed a methodology and implementation (see `anearis` Python package) for automated emissions harmonization for IAMs, which mostly contributes to improving the situation where harmonization is carried out separately by individual modeling teams with different methods. However, the `anearis` package described by the authors could not be found on `conda-forge` or `PyPi` for installation. Moreover, the scope of this work does not require advanced harmonization given that only global emissions (GHG and CO_2) must be harmonized. Consequently, emissions harmonization in this study is inspired from [Gidden et al., 2018], but not implemented through the `anearis` Python package (see future works discussion in Section 4.3.3).

In particular, both *constant* and *reduced offset* methods are applied for global emissions harmonization based on historical data (see Section 4.3.1). The use of reduced offset method for the harmonization ensures that in the presence of negative emissions, the first year of negative emissions is preserved (together with the emissions after that year). In fact, the authors in [Gidden et al., 2018] highlight how important it is for trajectories with negative emissions to match as closely as possible the timing and total magnitude of negative emissions. The emissions harmonization based on the offset method is implemented according to the following equations,

$$\begin{cases} m^h(t) = h(t) \qquad (\text{for } t_{m,0} \leq t \leq t_h) \\ m^h(t) = m(t) + \underbrace{\frac{1}{(t_{conv} - t_h)} \underbrace{\sum_{t_i = t_{m,0}}^{t_h} (m(t_i) - h(t_i))}_{\text{cumulative difference}}}_{\text{yearly correction}} \qquad (\text{for } t_h < t \leq t_{m,f}) \end{cases} \tag{4}$$

where $h(t)$ is the annual historical emissions in year t (as defined in Section 4.3.1), $m(t)$ is the annual emissions of the model-scenario in year t, $m^h(t)$ is the harmonized annual emissions of the model-scenario in year t, $t_{m,0}$ is the model base year, $t_{m,f}$ is the time horizon of the model (last year reported data, i.e., 2100), t_h is the harmonization year, and t_{conv} is the convergence year where the harmonized emissions converge to the original model-scenario emissions. For the *reduced offset*, t_{conv} is set to the first year or negative emissions whereas for the *constant offset*, $t_{conv} = t_{m,f}$. In practice, if model-scenario emissions are lower than historical emissions over the period $t_{m,0}$ to t_h, the yearly correction becomes negative. In that case, setting t_{conv} to the first year of negative emissions is not a sufficient condition to ensure that harmonized emissions have the same first year negative emissions. In fact, if the yearly correction is greater (in absolute terms) than the emissions in a previous year, then the first year of negative emissions will be reached earlier in harmonized emissions. Consequently, t_{conv} is iteratively decreased (one year at a time) to ensure that the original year of first negative emissions is preserved after emissions harmonization. Note that a log data file is generated by the code in `pyaesa` after harmonization, which provides for each scenario the harmonization method applied, the yearly correction, the final value of t_{conv}, and the error on both harmonized cumulative emissions (from $t_{m,0}$ to $t_{m,f}$) and first year of negative emissions.

Additional details regarding the harmonization process are provided in Figure 7, Figure 8, and Figure 9 for $t_h = t_{s,0} = 2019$. More specifically, Figure 8(a) shows that cumulative GHG emissions (WO AFOLU) from all models considered are statistically relatively well aligned with historical emissions (WO AFOLU). This is not necessarily the case for the three other variables where model cumulative emissions are statistically (i) higher for GHG and CO_2 emissions including AFOLU, and (ii) lower for CO_2 emissions excluding AFOLU. An explanation for (i) could be that historical emissions including AFOLU reported in PRIMAP-hist may be underestimated, as discussed in Section 4.3.1. Figure 8(b) shows that yearly correction applied during the harmonization are bounded between -1.6 and +0.7 $GtCO_2eq\ yr^{-1}$, while it can go down to -1.7 $GtCO_2eq\ yr^{-1}$ and up to +5 $GtCO_2eq\ yr^{-1}$ in for other variables. All details are available in the harmonization log file generated by `pyaesa`. Figure 9 shows that the total cumulative effect of harmonization is relatively small, which is similar to the finding of [Kikstra et al., 2022] for the period 2020-2100 (note that the study carries out emissions infilling on top of harmonization, whereas this work is limited to emissions harmonization).

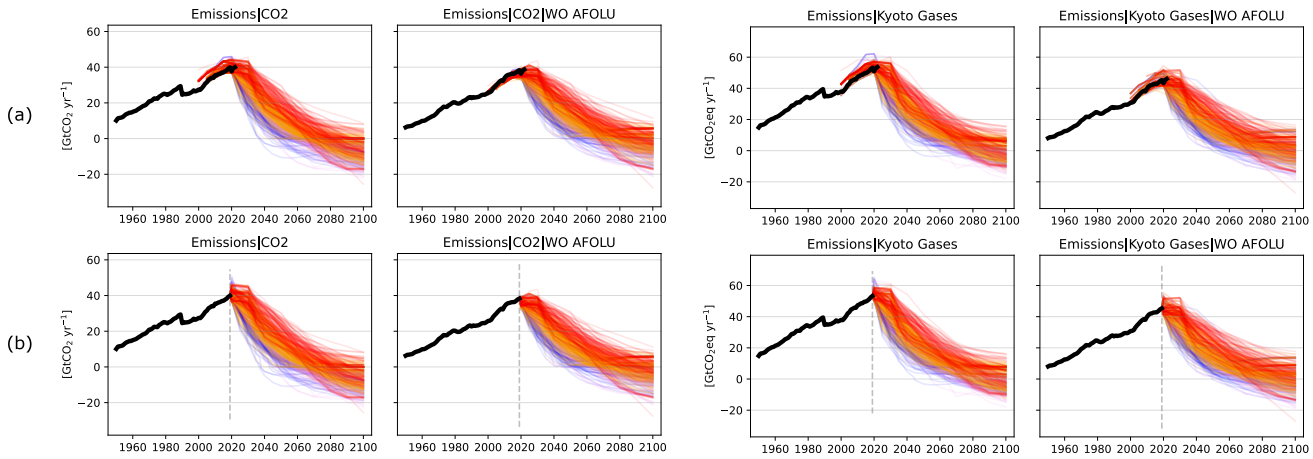

Figure 7: (a) Emissions pathways without harmonization and historical emissions for the corresponding variable. (b) Harmonized emissions pathways ($t_h = t_{s,0} = 2019$) based on historical emissions estimated in Section 4.3.1.

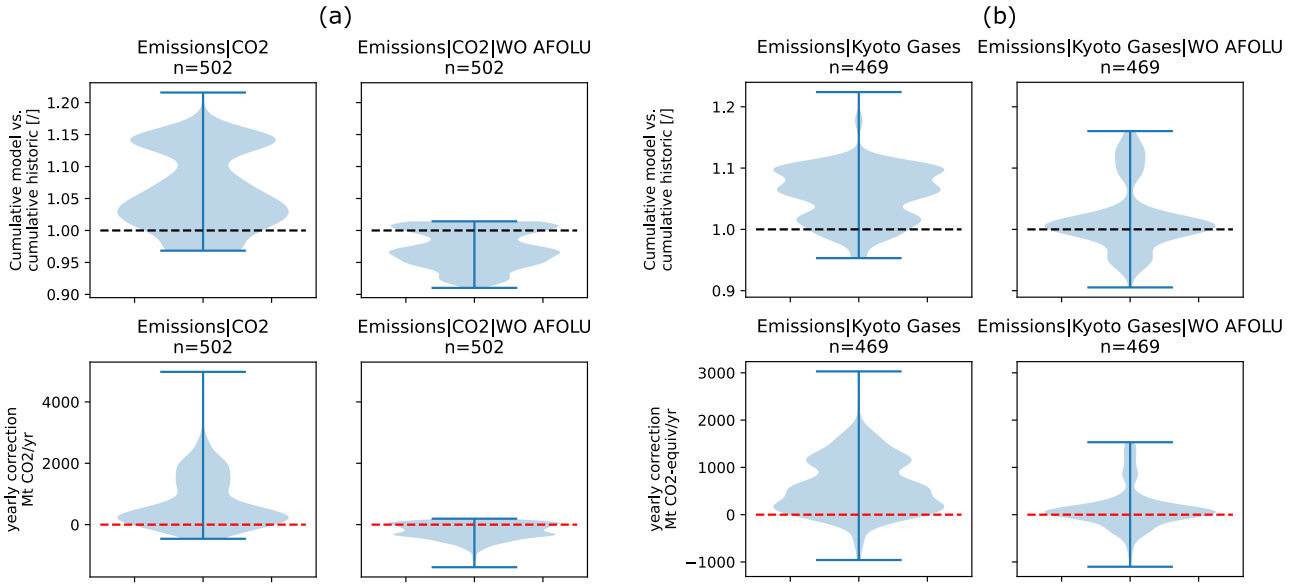

Figure 8: Details regarding the harmonization process for the period 2019-2100. For (a) CO_2 emissions and (b) GHG emissions (both excluding and including AFOLU emissions), the distribution is provided for the ratio between cumulative emissions of the models and historical emissions until the harmonization year t_h, and the resulting yearly correction applied from t_h to t_{conv}. The number of scenarios (pathways) considered is provided for each variable (n=#).

4.3.2.4 Estimation of gross emissions

Estimating net budgets for CO_2 and GHG emissions over a given time period is useful, but it has a major drawback for applications in AESA. As discussed in the manuscript, justice distributive theories used for sharing principles during the allocation are based on ethics for *distributing* a limited resource (here a quantity of emissions), not for distributing an *obligation* to sequestrate emissions as it would be the case with negative yearly emissions (or negative budgets). Consequently, we propose to split gross and negative emissions based on harmonized net emissions. This approach is similar to the approach pro-

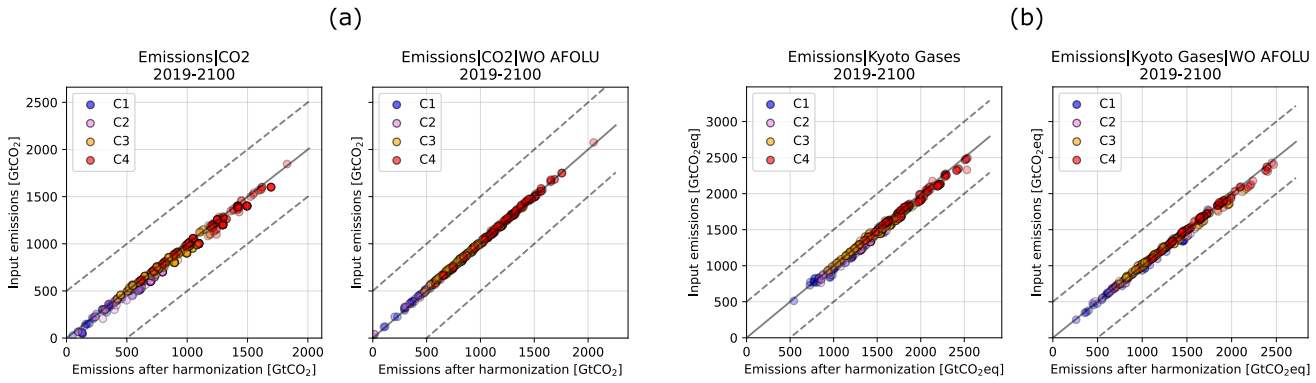

Figure 9: Effect of the harmonization process on (a) CO_2 emissions budgets and (b) GHG emissions budgets (both excluding and including AFOLU emissions) for the period 2019-2100.

posed in [Lejeune et al., 2026] for the hydrogen production sub-sector (within the energy sector), although different as it aims to be applicable for global carrying capacities for several countries and sectors (not only for a specific sector). The approach proposed in this work is further detailed in the following sections.

Negative emissions and carbon sequestration

First, negative emissions are estimated based on AR6 explorer variables for carbon sequestration. More than 30 variables are available in the AR6 explorer for carbon sequestration, but several of them are sub-contributions that come down to six subsets, i.e., CCS (carbon capture and storage), Direct Air Capture, Enhanced Weathering, Feedstocks, Land Use, Other. Among those, Carbon Sequestration|CCS is of a specific a nature as it covers total carbon dioxide emissions from bioenergy use and fossil fuel use captured and stored in geological deposits and the deep ocean, *before* being released in the atmosphere, as detailed in Table 4. On the contrary, variables for Direct Air Capture, Enhanced Weathering, Feedstocks, Land Use, and Other capture solutions that aims at sequestrating carbon from the atmosphere *after* being released.

This work hence defines two subsets of carbon sequestration variables as detailed below, i.e., Carbon Sequestration|Total and Carbon Sequestration|Subtotal_seq. An overview of all carbon sequestrations contributions split by categories is provided in Figure 10. This clearly highlights the high reliance on carbon sequestration in emissions pathways, mostly after 2030-2040. Moreover, it appears clearly that biggest contributions to Sequestration|Subtotal_seq are from Carbon Sequestration|Land Use and Carbon Sequestration|Direct Air Capture, whereas biggest contributions for Carbon Sequestration|Total is Sequestration|CCS.

Table 7: Sequestration variables.

Variable	**Expression**
Carbon Sequestration|Subtotal_seq	Carbon Sequestration|Direct Air Capture + Carbon Sequestration|Enhanced Weathering + Carbon Sequestration|Feedstocks + Carbon Sequestration|Land Use + Carbon Sequestration|Other
Carbon Sequestration|Total	Carbon Sequestration|Subtotal_seq + Carbon Sequestration|CCS

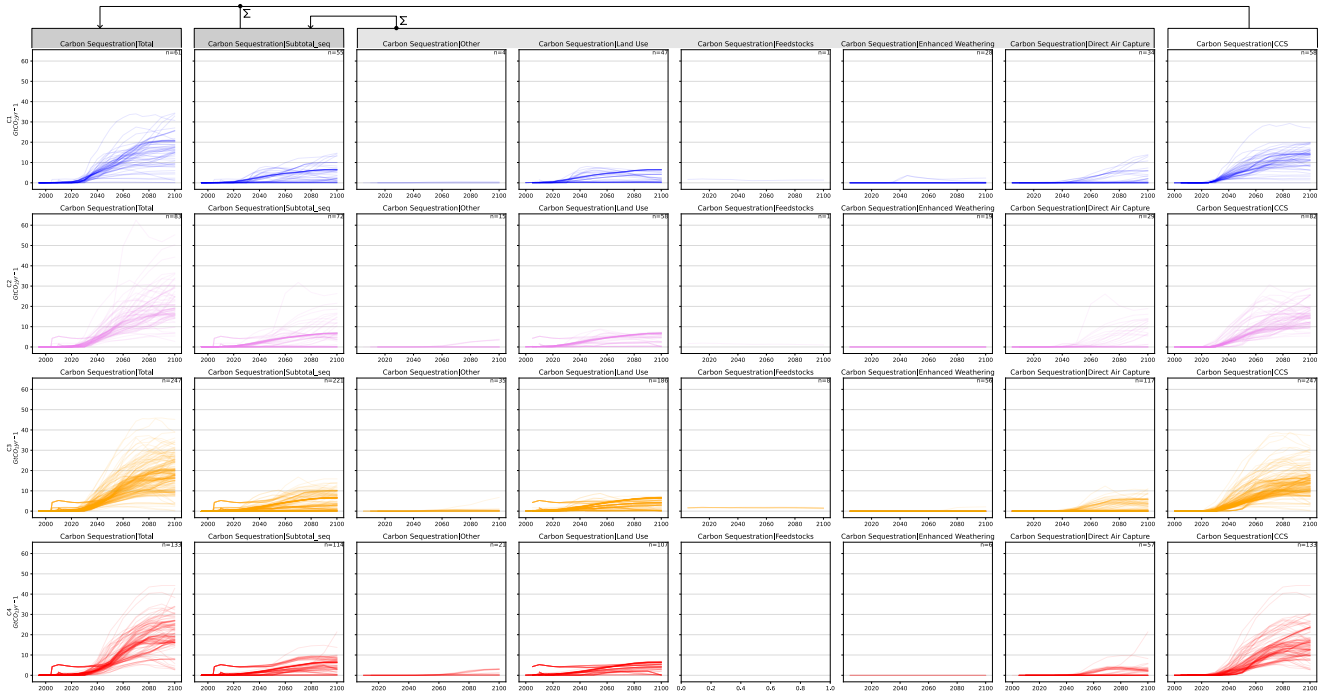

Figure 10: Carbon sequestration contributions by categories (C1 to C4) for all models-scenarios considered in this work, i.e., with data available in $t_{s,0} = 2019$. Data is shown over the full models definition period (until 2100). This improves the understanding of the different sequestration contributions for both Carbon Sequestration|Subtotal_seq and Carbon Sequestration|Total. Note that in the AR6 explorer, all carbon sequestration variables should be reported as positive numbers. However, this is not the case for all scenarios. In fact, 66 scenarios (all from IMAGE3.0 and IMAGE3.0.1 models) are filtered out as they have carbon sequestration negative values.

Gross and gross$_{alt}$ emissions

Once carbon sequestrations have been computed, gross emissions are estimated for each harmonized variable by removing carbon sequestration contributions. Two approaches are considered based on the two subsets of carbon sequestration variables, i.e., Carbon Sequestration|Total and Carbon Sequestration|Subtotal_seq. On one side, removing all carbon sequestration (Carbon Sequestration|Total) provides the gross emissions. On the other side, removing all carbon sequestration except CCS contributions (Carbon Sequestration|Subtotal_seq) provides an alternative gross emissions variable (gross_alt), accounting for sequestration if it is applied directly at the source of emissions, but not for solutions that aims at sequestrating carbon from the atmosphere as it is the case for contributions from Direct Air Capture, Enhanced Weathering, Feedstocks, Land Use, and Other.

Once gross (and gross_alt) emissions have been estimated for all available scenarios, only the ones that are always positive are considered. This ensures that both emissions pathways *and* budgets will be always positive and usable as global carrying capacities for AESA allocation. It is important that associated carbon sequestration emissions and budgets are always considered together with the gross (and gross_alt) emissions, as the *obligation* to sequestrate emissions must also be allocated. Nevertheless, this topic is still scarcely addressed in current AESA literature and must be discussed in future works.

Table 8: Gross and gross$_{alt}$ variables.

Variable	Expression
Emissions(gross)|CO2	Emissions|CO2 - Carbon Sequestration|Total
Emissions(gross_alt)|CO2	Emissions|CO2 - Carbon Sequestration|Subtotal_seq
Emissions(gross)|CO2|WO AFOLU	Emissions|CO2|WO AFOLU - Carbon Sequestration|Total
Emissions(gross_alt)|CO2|WO AFOLU	Emissions|CO2|WO AFOLU - Carbon Sequestration|Subtotal_seq
Emissions(gross)|Kyoto Gases	Emissions|Kyoto Gases - Carbon Sequestration|Total
Emissions(gross_alt)|Kyoto Gases	Emissions|Kyoto Gases - Carbon Sequestration|Subtotal_seq
Emissions(gross)|Kyoto Gases|WO AFOLU	Emissions|Kyoto Gases|WO AFOLU - Carbon Sequestration|Total
Emissions(gross_alt)|Kyoto Gases|WO AFOLU	Emissions|Kyoto Gases|WO AFOLU - Carbon Sequestration|Subtotal_seq

Note that Emissions|CO2, Emissions|CO2|WO AFOLU, Emissions|Kyoto Gases, and Emissions|Kyoto Gases|WO AFOLU variables are renamed to Emissions(net)|CO2, Emissions(net)|CO2|WO AFOLU, Emissions(net)|Kyoto Gases, and Emissions(net)|Kyoto Gases|WO AFOLU in `pyaesa` for the sake of clarity.

4.3.2.5 Comparison of net emissions budgets to scientific literature

This subsection compares the (net) budgets obtained for the periods 2010-2100 and 2020-2100 (based on the methodology described in the previous sections) with results from the scientific literature. This aims at demonstrating that the approach provides similar results compared to two different studies, over two different periods.

Comparison for 2010-2100

As pointed out in [Gebara and Laurent, 2023], the study of [Robiou du Pont et al., 2017] is likely one of the most comprehensive work providing carbon budget estimates including all GHGs based on various scenarios aligning with the 1.5°C and 2°C targets. Mean values reported in that study focused on the 2010-2100 period and are based on a selection of pathways and scenarios from the IPCC-AR5 database. The authors in [Robiou du Pont et al., 2017, Gebara and Laurent, 2023] report 1749 (1260-2598) $GtCO_2eq$ (2C-pre2020peak scenario set) and 1156 (481-1791) $GtCO_2eq$ (1.5C-pre2020peak scenario set) for the period 2010-2100 (see Table 2 in their study). Note that their budgets exclude LULUCF emissions and exclude bunkers emissions, whereas budgets in this study excludes LULUCF (*and* agriculture!) emissions while including bunker emissions[21]. According to the description of their scenario set in [Robiou du Pont et al., 2017] (see Table 1 in their study), the best comparison for the 2C-pre2020peak is assumed to be the C3 category. For the 1.5C-pre2020peak scenario set, both C1 and C2 can fit. The comparison is illustrated in Figure 11 and exact values are provided in Table 9. From this comparison, budgets estimated in this work are aligned with the ones provided in [Robiou du Pont et al., 2017] (and used in [Gebara and Laurent, 2023]) for the 1.5°C target (categories C1 and C2). More specifically, budgets in this work seem slightly underestimated (about 8%) compared to [Robiou du Pont et al., 2017] for C3, while being slightly overestimated (about 5%) for C1. The comparison with category C2 shows that budgets from this study are overestimated (about 20%) compared to [Robiou du Pont et al., 2017], but this can mostly be explained by the fact that their 1.5C-pre2020peak scenario is better matched with category C1.

[21] As detailed in Section 4.3.1, bunker emissions represent less than 3% of total GHG emissions, which is therefore relatively marginal

Table 9: Summary of (net) GHG budgets for 2010 to 2100, sorted by category (climate pathway) and SSPs.

Category*	**SSP familly**	**Models included**	**Scenarios included**	**GHG budget**$^\circ$ $[GtCO_2eq]$ (2010-2100)
C1	all available	15	58	**1211 (643-2115)**
C2	all available	15	68	**1376 (855-1968)**
C3	all available	19	207	**1614 (1126-2523)**
C4	all available	13	106	2031 (1085-2854)

$\star$: *C1*: limit warming to 1.5°C (>50%) with no or limited overshoot, *C2*: return warming to 1.5C (>50%) after a high overshoot', *C3*: limit warming to 2C (>67%), *C4*: limit warming to 2C (>50%), *C5*: limit warming to 2.5C (>50%), *C6*: limit warming to 3C (>50%), *C7*: limit warming to 4°C (>50%).

$\circ$: Budgets are provided excluding AFOLU emissions (and including IAS emissions) for both Kyoto Gases (GHG) emissions.

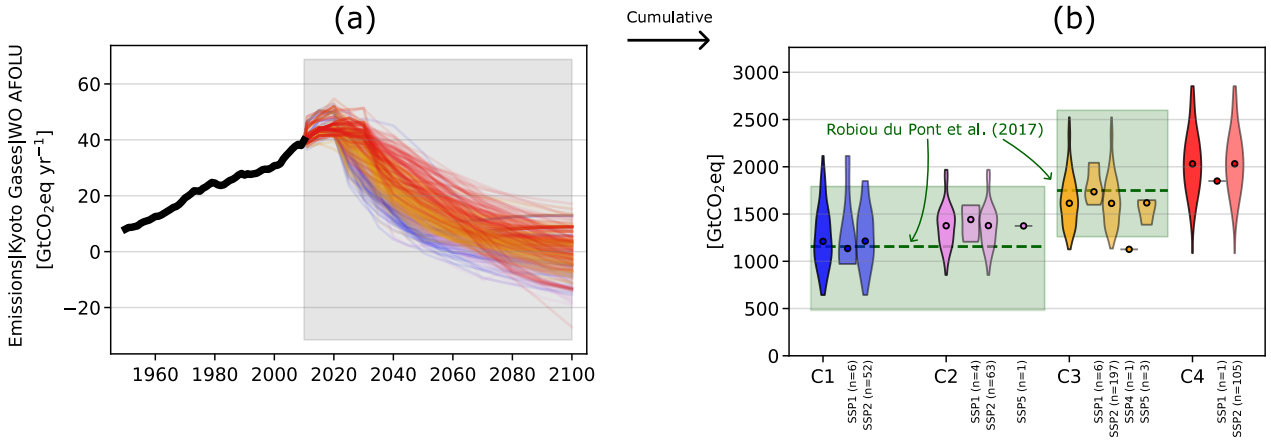

Figure 11: (a) Results of the emissions harmonization for the period 2010-2100 with respect to historical emissions described in Section 4.3.1. (b) Comparison between obtained net budgets for 2010-2100 (based on harmonized emissions depicted in (a)) and net budgets from the scientific literature [Robiou du Pont et al., 2017] (depicted in dark green, the median in dashed line and uncertainty in shaded area).

Comparison for 2020-2100

Another key study published in 2022 [Kikstra et al., 2022] provides in-depth analysis and details regarding the "climate-assessment" workflow and methods used in the AR6 Working Group III (WGIII). In particular, the study often provides a clear split by categories for emissions harmonization and infilling, evolution of the global mean surface temperature (GSAT), or Kyoto Gases emissions budgets over the period 2020-2100 (see Figure 8 in their study). However, emissions budgets distributions are not provided explicitly in the study for each category. The comparison here is therefore mainly limited to comparing the range of budgets for categories C1 to C4, as depicted in Figure 12. It is likely that the study [Kikstra et al., 2022] report Kyoto Gases emissions including AFOLU emissions, but this was not stated explicitly. Results are therefore compared both including and excluding AFOLU emissions. This shows that estimated harmonized budgets for Kyoto Gases emissions over the period 2020-2100 are in a very similar range, i.e., 500 to 2500 $GtCO_2eq$. Nonetheless, their study [Kikstra et al., 2022] carries out infilling of missing emissions together with emissions harmonization, whereas this work only includes emissions harmonization to align all models-scenarios with historical emissions at a given harmonization year $t_h = t_{s,0} = 2020$.

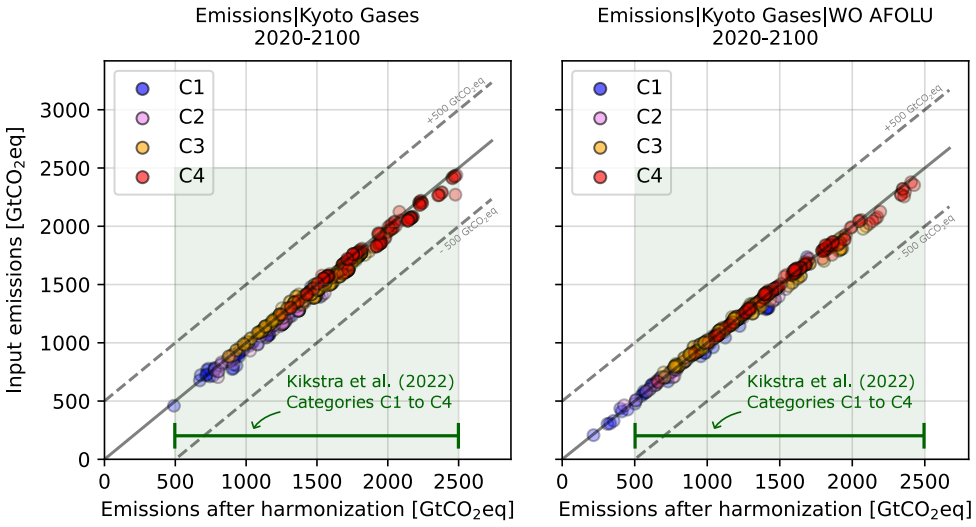

Figure 12: Results of the emissions harmonization for the period 2020-2100 with respect to historical emissions described in Section 4.3.1. Kyoto Gases emissions budgets per category are reported similarly to the study in the scientific literature [Kikstra et al., 2022] to allow for a qualitative visual comparison. The range of Kyoto Gases emissions budgets from [Kikstra et al., 2022] for categories C1 to C4 is depicted by the dark green shaded area.

4.3.2.6 Budgets for the study period (2019-2060) and annual harmonized emissions

.

This subsection provides the emissions budgets for the period of interest in this study, i.e., 2019 to 2060. The pathways (annual values) for each scenario is also provided by the Python package `pyaesa`. Budgets are computed based on harmonized emissions as depicted in Figure 13(a), assuming that every scenario has the same weight. Estimated budgets are illustrated in Figure 13(b) and exact values can be obtained from `pyaesa`. Given that the study period ends before 2100 (time horizon for the models), the *remaining* budgets for 2061-2100 are also provided in Figure 13(c) to put in perspective the reduction efforts that will be necessary after $t_{s,f}$ (i.e., 2060). Budgets for the study period increases with the category (median from C1 to C4), although there is significant overlap between the budgets of the categories. Remaining budgets also show a similar trend, and all of the four categories includes (to some extent) negative emissions after 2060. Total emissions are always higher for the GHG emissions, as Kyoto gazes are accounted for on top of CO_2. The greater variation is assumed to be (partly) due to the different lifetimes and warming potentials for the different GHG.

The Python package `pyaesa` can provide emissions budgets for the three approaches (i.e., *net* budgets, *gross* budgets, and $gross_{alt}$ budgets), for both GHG and CO_2 emissions (including and excluding AFOLU emissions). This is illustrated in Figure 13 for GHG emissions only, for the sake of conciseness.

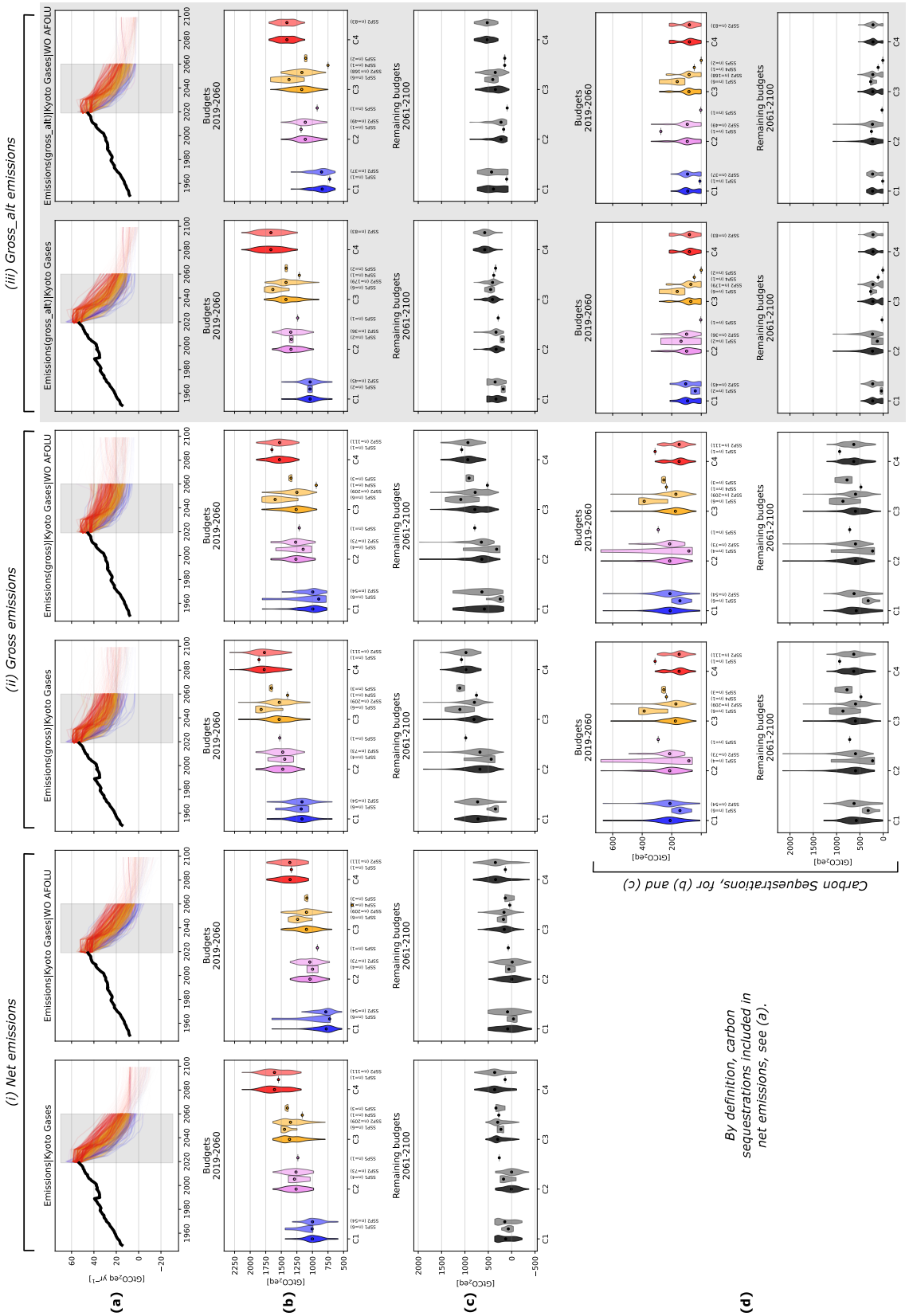

Figure 13: (a) Results of the GHG emissions harmonization for the period 2019-2060 with respect to historical emissions described in Section 4.3.1. (b) GHG budgets estimated for the study period 2019-2060. (c) Remaining GHG budgets from 2061 to 2100.

4.3.2.7 Uncertainty and Monte Carlo sampling approach

Similarly to the full SOS definition in the planetary boundary framework, the IAM-SSP-Climate pathway approach also embeds inherent uncertainty. In fact, there are several models proposing several scenarios for each category, which turns out into variability in budgets estimation for a defined period of time. This can eventually be propagated to the estimation of the assigned share of carrying capacities. Nevertheless, because budgets distribution overlaps, a ratio between the carrying capacity for category "Cx" and category "Cy" cannot be easily obtained, on the contrary to carrying capacities defined in the planetary boundary framework as detailed in Section 2.6. In the case of dynamic carrying capacities, uncertainty is therefore propagated through Monte Carlo simulations, according to uncertainty sources included by the practitioner, i.e., category uncertainty and inter-model uncertainty.

In practice, one emission pathway is drawn from the list of available scenarios (for a given category and a given SSP) at each Monte Carlo simulation. Yet, the sampling approach for the Monte Carlo simulation must be discussed given that it is also a modeling choice. In particular, two main approaches can be used for the Monte Carlo simulation [Rosenbaum et al., 2017]. One approach (the simplest) is the *simple random sampling*, (SRS) which consists in sampling randomly in the list of (harmonized) model-scenarios available (while ensuring matching with SSP family with the numerator of the ASR). Given that certain family models are more represented then others, a SRS approach lead to an unbalanced representation of models (favoring models that report more scenarios). Yet, this approach has the advantage to consider the list of scenarios available in the AR6-public database as a reference, without adding an extra layer of weighting between scenarios. The second approach is the *Latin hypercube sampling* (LHS), which consists in first dividing a distribution into segments of equal probability and randomly samples one value from each segment [Rosenbaum et al., 2017]. In the present case, this translates in giving the same probability of sampling to each model, and then assume random sampling of scenarios within each model. This approach therefore balances model representation, but leads to an unbalanced sampling of scenarios. The effect of adopting a SRS or a LHS sampling approach for the Monte Carlo is depicted[22] in Figure 14.

For the case study of interest in this work (2019-2060, Emissions(gross_alt)|Kyoto Gases|WO AFOLU), this shows that about 19% of the scenarios are over-represented in LHS compared to SRS (up to a factor 10×), while the rest of the scenarios are under-represented (between a factor 1× to 0.1×) compared to SRS. Yet, this has a limited impact on the final distributions of the estimated budgets, as shown in Figure 14. In fact, budgets median vary in the extreme case from -10% to +5% if the LHS approach is selected[23]. The SRS sampling method is therefore favored in this work, for its simplicity and because this has very little impact on the estimated budgets.

[22] Figure 14 is only provided here for GHG variables, but the same figure can be obtained for CO_2 variables via `pyaesa`.

[23] Note that depending on the study period and depending on the variable selected, variation can be more significant, e.g., -20% or +40%. This motivates the systematic analysis of the Monte Carlo sampling method, as proposed in this work

4.3.3 Limitations and future works

Although this work provides as systematic and flexible approach to define dynamic carrying capacities for GHG and CO_2 emissions budgets, it also has limitations as listed below.

This work defines carrying capacities for GHG emissions (and CO_2 emissions), but carrying capacities for individual gazes in GHG emissions are not considered. This may be further improved in the future, as GHG have different lifetimes which can leads for instance to non-linear behaviors that are currently simplified when considering a GWP100 LCIA method.

Interactions between Earth system processes are not considered in carrying capacities definition. They are all considered as independent, although they have known interactions [Lejeune et al., 2026]. The quantification of the interactions between boundaries remains a major challenge in the current literature, even though recent studies have shown that additional or more extensive transgression of one planetary boundary can change risk gradients for other boundaries [Richardson et al., 2023].

The authors in [Gidden et al., 2018] point out two families of methods for harmonization, i.e., ratio-based and offset-based. Implementing a ratio-based method could be investigated as future work, together with integrating the use of `anearis` to perform the harmonization step. The current implementation already use the IAM community format for data processing, which should ease the implementation of suggested future works.

Finally, although emissions harmonization is implemented in this work, infilling of missing emissions was not carried out. This could be done in future works, as the infilling process in the AR6 was performed using an open-source Python software package called 'silicone' [Lamboll et al., 2020], according to [Kikstra et al., 2022]. Infilled emissions variables also exist in the AR6 databases, which could be further investigated to understand wether those variables could be used instead of the selected variables in Table 4.

In most cases, these limitations are in line with limitations pointed out in literature. Future works can improve the proposed approach and eventually, update the implementation in Python package `pyaesa` once steps have been validated. This would ultimately contribute to an harmonized definition of global dynamic carrying capacities for climate change in AESA studies.

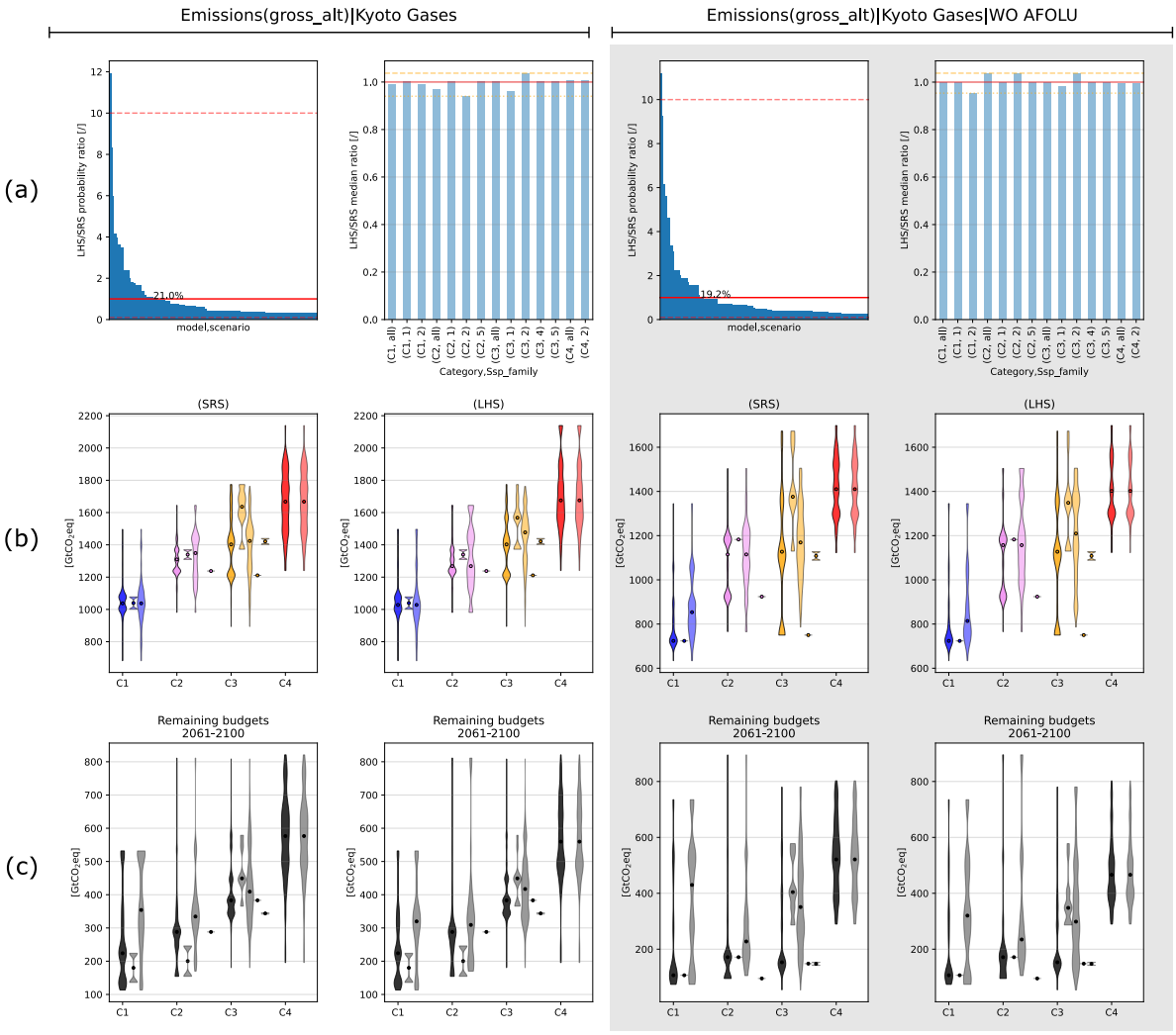

Figure 14: (a) Ratio between LHS and SRS probability of being selected in Monte Carlo simulation and the resulting GHG budgets median for each model-scenario. (b) Impact of the Monte Carlo sampling approach on the estimated GHG budgets for the simple random sampling (SRS) approach and the Latin hypercube sampling (LHS) approach. (c) Impact of the Monte Carlo sampling approach on the estimated remaining GHG budgets from 2061 to 2100.

References

[Biermann, 2012] Biermann, F. (2012). Planetary boundaries and earth system governance: Exploring the links. *Ecological Economics*, 81:4–9. https://doi.org/10.1016/j.ecolecon.2012.02.016 (accessed May 2026).

[Bjørn and Hauschild, 2015] Bjørn, A. and Hauschild, M. Z. (2015). Introducing carrying capacity-based normalisation in lca: framework and development of references at midpoint level. *The International Journal of Life Cycle Assessment*, 20:1005–1018. https://doi.org/10.1007/s11367-015-0899-2.

[Bjørn et al., 2025] Bjørn, A., Paulillo, A., Sanye, M. E., Valeria, D., Vea, E., Hauschild, M. Z., Sala, S., et al. (2025). Guidance for applying absolute environmental sustainability assessment on activities at different scales (beta version). https://dx.doi.org/10.2760/7677803.

[Brand-Correa and Steinberger, 2017] Brand-Correa, L. I. and Steinberger, J. K. (2017). A framework for decoupling human need satisfaction from energy use. *Ecological Economics*, 141:43–52. https://doi.org/10.1016/j.ecolecon.2017.05.019.

[Byers et al., 2022] Byers, E., Krey, V., Kriegler, E., Riahi, K., Schaeffer, R., Kikstra, J., Lamboll, R., Nicholls, Z., Sandstad, M., Smith, C., van der Wijst, K., Al Khourdajie, A., Lecocq, F., Portugal-Pereira, J., Saheb, Y., Stromann, A., Winkler, H., Auer, C., Brutschin, E., Gidden, M., Hackstock, P., Harmsen, M., Huppmann, D., Kolp, P., Lepault, C., Lewis, J., Marangoni, G., Müller-Casseres, E., Skeie, R., Werning, M., Calvin, K., Forster, P., Guivarch, C., Hasegawa, T., Meinshausen, M., Peters, G., Rogelj, J., Samset, B., Steinberger, J., Tavoni, M., and van Vuuren, D. (2022). AR6 Scenarios Database. https://doi.org/10.5281/zenodo.5886911 (accessed March 2026).

[Clausen et al., 2025] Clausen, C. A., Hauschild, M. Z., and Bjørn, A. (2025). Absolute environmental sustainability assessments of long-lived systems: A review of challenges with the representation of time and future research directions. *Sustainable Production and Consumption*. https://doi.org/10.1016/j.spc.2025.06.006.

[Dao et al., 2018] Dao, H., Peduzzi, P., and Friot, D. (2018). National environmental limits and footprints based on the planetary boundaries framework: The case of switzerland. *Global environmental change*, 52:49–57. https://doi.org/10.1016/j.gloenvcha.2018.06.005.

[Fricko et al., 2017] Fricko, O., Havlik, P., Rogelj, J., Klimont, Z., Gusti, M., Johnson, N., Kolp, P., Strubegger, M., Valin, H., Amann, M., et al. (2017). The marker quantification of the shared socioeconomic pathway 2: A middle-of-the-road scenario for the 21st century. *Global Environmental Change*, 42:251–267. https://doi.org/10.1016/j.gloenvcha.2016.06.004.

[Friedlingstein et al., 2024] Friedlingstein, P., O'sullivan, M., Jones, M. W., Andrew, R. M., Hauck, J., Landschützer, P., Le Quéré, C., Li, H., Luijkx, I. T., Olsen, A., et al. (2024). Global carbon budget 2024. *Earth System Science Data Discussions*, 2024:1–133. https://doi.org/10.5194/essd-17-965-2025.

[Galán-Martín et al., 2021] Galán-Martín, Á., Tulus, V., Díaz, I., Pozo, C., Perez-Ramirez, J., and Guillen-Gosalbez, G. (2021). Sustainability footprints of a renewable carbon transition for the petrochemical sector within planetary boundaries. *One Earth*, 4(4):565–583. https://doi.org/10.1016/j.oneear.2021.04.001.

[Galaz et al., 2012] Galaz, V., Biermann, F., Folke, C., Nilsson, M., and Olsson, P. (2012). Global environmental governance and planetary boundaries: an introduction. https://doi.org/10.1016/j.ecolecon.2012.02.023 (accessed May 2026).

[Gebara and Laurent, 2023] Gebara, C. H. and Laurent, A. (2023). National sdg-7 performance assessment to support achieving sustainable energy for all within planetary limits. *Renewable and Sustainable Energy Reviews*, 173:112934. https://doi.org/10.1016/j.rser.2022.112934.

[Gidden et al., 2018] Gidden, M. J., Fujimori, S., van den Berg, M., Klein, D., Smith, S. J., van Vuuren, D. P., and Riahi, K. (2018). A methodology and implementation of automated emissions harmonization for use in integrated assessment models. *Environmental Modelling & Software*, 105:187–200. https://doi.org/10.1016/j.envsoft.2018.04.002.

[Guinée et al., 2022] Guinée, J. B., de Koning, A., and Heijungs, R. (2022). Life cycle assessment-based absolute environmental sustainability assessment is also relative. *Journal of Industrial Ecology*, 26(3):673–682. https://doi.org/10.1111/jiec.13260.

[Gütschow et al.,] Gütschow, J., Jeffery, L., Gieseke, R., Gebel, R., Stevens, D., Krapp, M., and Rocha, M. The PRIMAP-hist national historical emissions time series (1750-2023)(v2. 6.1, updated March 2025). https://doi.org/10.5281/zenodo.15016289.

[Gütschow et al., 2025] Gütschow, J., Busch, D., and Pflüger, M. (2025). The primap-hist national historical emissions time series (1750-2024) v2.7.

[Hadziosmanovic et al., 2022] Hadziosmanovic, M., Lloyd, S. M., Bjørn, A., Paquin, R. L., Mengis, N., and Matthews, H. D. (2022). Using cumulative carbon budgets and corporate carbon disclosure to inform ambitious corporate emissions targets and long-term mitigation pathways. *Journal of Industrial Ecology*, 26(5):1747–1759. https://doi.org/10.1111/jiec.13322 (accessed June 2026).

[Hansen et al., 2013] Hansen, J., Kharecha, P., Sato, M., Masson-Delmotte, V., Ackerman, F., Beerling, D. J., Hearty, P. J., Hoegh-Guldberg, O., Hsu, S.-L., Parmesan, C., et al. (2013). Assessing "dangerous climate change": Required reduction of carbon emissions to protect young people, future generations and nature. *PloS one*, 8(12):e81648. https://doi.org/10.1371/journal.pone.0081648.

[Hellweg et al., 2023] Hellweg, S., Benetto, E., Huijbregts, M. A., Verones, F., and Wood, R. (2023). Life-cycle assessment to guide solutions for the triple planetary crisis. *Nature Reviews Earth & Environment*, 4(7):471–486. https://doi.org/10.1038/s43017-023-00449-2.

[IIASA, 2025a] IIASA (2025a). ENAGE Scenario explorer. https://iiasa.ac.at/models-tools-data/engage-scenario-explorer (accessed August 2025).

[IIASA, 2025b] IIASA (2025b). Pyam: Query data from the IIASA database infrastructure. https://pyam-iamc.readthedocs.io/en/stable/tutorials/iiasa.html (accessed August 2025).

[Jabbour and Hunsberger, 2014] Jabbour, J. and Hunsberger, C. (2014). Visualizing relationships between drivers of environmental change and pressures on land-based ecosystems. *Natural Resources*, 5(4):146. http://dx.doi.org/10.4236/nr.2014.54015 (accessed April 2026).

[Kikstra et al., 2022] Kikstra, J. S., Nicholls, Z. R., Smith, C. J., Lewis, J., Lamboll, R. D., Byers, E., Sandstad, M., Meinshausen, M., Gidden, M. J., Rogelj, J., et al. (2022). The ipcc sixth assessment report wgiii climate assessment of mitigation pathways: from emissions to global temperatures. *Geoscientific Model Development*, 15(24):9075–9109. https://doi.org/10.5194/gmd-15-9075-2022.

[Lamboll et al., 2020] Lamboll, R. D., Nicholls, Z. R., Kikstra, J. S., Meinshausen, M., and Rogelj, J. (2020). Silicone v1. 0.0: an open-source python package for inferring missing emissions data for climate change research. *Geoscientific Model Development*, 13(11):5259–5275. https://doi.org/10.5194/gmd-13-5259-2020 (accessed May 2026).

[Lejeune et al., 2026] Lejeune, M., Kara, S., Hauschild, M. Z., Shahrabifarahani, S., and Daiyan, R. (2026). Pathways to global hydrogen production within planetary boundaries. *Nature Communications*, 17(1):3521. https://doi.org/10.1038/s41467-026-70168-x.

[Lind and Andersen, 2024] Lind, A. and Andersen, L. C. (2024). From planetary boundaries to planetary politics. https://concito.dk/files/media/document/Brief%202_Planetary%20Boundaries%20Global%20to%20national%20boundaries_2.pdf (accessed August 2025).

[Lund et al., 2025] Lund, M. N., Schjerbeck, A. K., and Bjørn, A. (2025). Using absolute environmental sustainability assessment and mid-to-endpoint modeling to identify the most relevant impact categories to include in a building lca. *Building and Environment*, 278:112985. https://doi.org/10.1016/j.buildenv.2025.112985.

[Meinshausen et al., 2020] Meinshausen, M., Nicholls, Z. R., Lewis, J., Gidden, M. J., Vogel, E., Freund, M., Beyerle, U., Gessner, C., Nauels, A., Bauer, N., et al. (2020). The shared socio-economic pathway (ssp) greenhouse gas concentrations and their extensions to 2500. *Geoscientific Model Development*, 13(8):3571–3605. https://doi.org/10.5194/gmd-13-3571-2020 (accessed May 2026).

[Meinshausen et al., 2011] Meinshausen, M., Smith, S. J., Calvin, K., Daniel, J. S., Kainuma, M. L., Lamarque, J.-F., Matsumoto, K., Montzka, S. A., Raper, S. C., Riahi, K., et al. (2011). The rcp greenhouse gas concentrations and their extensions from 1765 to 2300. *Climatic change*, 109(1):213. https://doi.org/10.1007/s10584-011-0156-z (accessed May 2026).

[Minx et al., 2021] Minx, J. C., Lamb, W. F., Andrew, R. M., Canadell, J. G., Crippa, M., Döbbeling, N., Forster, P. M., Guizzardi, D., Olivier, J., Peters, G. P., et al. (2021). A comprehensive and synthetic dataset for global, regional, and national greenhouse gas emissions by sector 1970–2018 with an extension to 2019. *Earth System Science Data*, 13(11):5213–5252. https://doi.org/10.5194/essd-13-5213-2021.

[Minx et al., 2022] Minx, J. C., Lamb, W. F., Andrew, R. M., Canadell, J. G., Crippa, M., Döbbeling, N., Forster, P., Guizzardi, D., Olivier, J., Pongratz, J., Reisinger, A., Rigby, M., Peters, G., Saunois, M., Smith, S. J., Solazzo, E., and Tian, H. (2022). A comprehensive and synthetic dataset for global, regional and national greenhouse gas emissions by sector 1970-2018 with an extension to 2019. https://doi.org/10.5281/zenodo.6483002.

[Persson et al., 2022] Persson, L., Carney Almroth, B. M., Collins, C. D., Cornell, S., De Wit, C. A., Diamond, M. L., Fantke, P., Hassellov, M., MacLeod, M., Ryberg, M. W., et al. (2022). Outside the safe operating space of the planetary boundary for novel entities. *Environmental science & technology*, 56(3):1510–1521. https://doi.org/10.1021/acs.est.1c04158.

[Puig-Samper et al., 2025] Puig-Samper, G., Owsianiak, M., Clavreul, J., Jeandaux, C., Prieur-Vernat, A., and Gondran, N. (2025). Quantifying uncertainties in absolute environmental sustainability assessment: A general framework applied to french electricity production. *Sustainable Production and Consumption*, 54:12–24. https://doi.org/10.1016/j.spc.2024.12.013.

[Riahi et al., 2017] Riahi, K., Van Vuuren, D. P., Kriegler, E., Edmonds, J., O'neill, B. C., Fujimori, S., Bauer, N., Calvin, K., Dellink, R., Fricko, O., et al. (2017). The shared socioeconomic pathways and their energy, land use, and greenhouse gas emissions implications: An overview. *Global environmental change*, 42:153–168. https://doi.org/10.1016/j.gloenvcha.2016.05.009.

[Richardson et al., 2023] Richardson, K., Steffen, W., Lucht, W., Bendtsen, J., Cornell, S. E., Donges, J. F., Drüke, M., Fetzer, I., Bala, G., Von Bloh, W., et al. (2023). Earth beyond six of nine planetary boundaries. *Science advances*, 9(37):eadh2458. https://doi.org/10.1126/sciadv.adh2458.

[Robiou du Pont et al., 2017] Robiou du Pont, Y., Jeffery, M. L., Gütschow, J., Rogelj, J., Christoff, P., and Meinshausen, M. (2017). Equitable mitigation to achieve the paris agreement goals. *Nature Climate Change*, 7(1):38–43. https://doi.org/10.1038/nclimate3186.

[Rockström et al., 2009a] Rockström, J., Steffen, W., Noone, K., Persson, Å., Chapin, F. S., Lambin, E. F., Lenton, T. M., Scheffer, M., Folke, C., Schellnhuber, H. J., et al. (2009a). A safe operating space for humanity. *nature*, 461(7263):472–475. https://doi.org/10.1038/461472a.

[Rockström et al., 2009b] Rockström, J., Steffen, W., Noone, K., Persson, Å., Chapin III, F. S., Lambin, E., Lenton, T. M., Scheffer, M., Folke, C., Schellnhuber, H. J., et al. (2009b). Planetary boundaries: exploring the safe operating space for humanity. *Ecology and society*, 14(2). https://www.jstor.org/stable/26268316.

[Rogelj et al., 2016] Rogelj, J., Schaeffer, M., Friedlingstein, P., Gillett, N. P., Van Vuuren, D. P., Riahi, K., Allen, M., and Knutti, R. (2016). Differences between carbon budget estimates unravelled. *Nature Climate Change*, 6(3):245–252. https://doi.org/10.1038/nclimate2868 (accessed May 2026).

[Rosenbaum et al., 2017] Rosenbaum, R. K., Georgiadis, S., and Fantke, P. (2017). Uncertainty management and sensitivity analysis. In *Life cycle assessment: theory and practice*, pages 271–321. Springer.

[Ryberg et al., 2018] Ryberg, M. W., Owsianiak, M., Clavreul, J., Mueller, C., Sim, S., King, H., and Hauschild, M. Z. (2018). How to bring absolute sustainability into decision-making: an industry case study using a planetary boundary-based methodology. *Science of the Total Environment*, 634:1406–1416. https://doi.org/10.1016/j.scitotenv.2018.04.075.

[Sakschewski et al., 2025] Sakschewski, B., Caesar, L., Andersen, L., Bechthold, M., Bergfeld, L., Beusen, A., Billing, M., Bodirsky, B. L., Botsyun, S., Dennis, D. P., Donges, J., Dou, X., Eriksson, A., Fetzer, I., Gerten, D., Häyhä, T., Hebden, S., Heckmann, T., Heilemann, A., Huiskamp, W., Jahnke, A., Kaiser, J., Kitzmann, N. H., Krönke, J., Kühnel, D., Laureanti, N. C., Li, C., Liu, Z., Loriani, S., Ludescher, J., Mathesius, S., Norström, A., Otto, F., Paolucci, A., Pokhotelov, D., Rafiezadeh Shahi, K., Raju, E., Rostami, M., Schaphoff, S., Schmidt, C., Steinert, N. J., Stenzel, F., Virkki, V., Wendt-Potthoff, K., Wunderling, N., Rockström, J., Kitzmann, N. H., Caesar, L., Sakschewski, B., and Rockström, J. (2025). Planetary Health Check 2025: A Scientific Assessment of the State of the Planet. Technical report, Potsdam Institute for Climate Impact Research (PIK). https://doi.org/10.48485/pik.2025.017.

[Sala et al., 2020] Sala, S., Crenna, E., Secchi, M., and Sanyé-Mengual, E. (2020). Environmental sustainability of european production and consumption assessed against planetary boundaries. *Journal of environmental management*, 269:110686. https://doi.org/10.1016/j.jenvman.2020.110686.

[Sanye et al., 2023] Sanye, M. E., Sala, S., et al. (2023). Consumption footprint and domestic footprint: Assessing the environmental impacts of eu consumption and production. https://dx.doi.org/10.2760/218540 (accessed May 2026).

[Serrano et al., 2025] Serrano, T., Meramo, S., Bjørn, A., Hauschild, M., Sukumara, S., and Sommer, M. O. (2025). Communicating the environmental impacts of individual actions in the context of planetary boundaries. *Sustainable Production and Consumption*, 56:420–430. https://doi.org/10.1016/j.spc.2025.03.021.

[Steffen et al., 2015] Steffen, W., Richardson, K., Rockström, J., Cornell, S. E., Fetzer, I., Bennett, E. M., Biggs, R., Carpenter, S. R., De Vries, W., De Wit, C. A., et al. (2015). Planetary boundaries: Guiding human development on a changing planet. *science*, 347(6223):1259855. https://doi.org/10.1126/science.1259855.

[Stranddorf et al., 2023] Stranddorf, L. K., Clavreul, J., Prieur-Vernat, A., and Ryberg, M. W. (2023). Evaluation of life cycle impacts of european electricity generation in relation to the planetary boundaries. *Sustainable Production and Consumption*, 39:414–424. https://doi.org/10.1016/j.spc.2023.05.026.

[Vázquez et al., 2023] Vázquez, D., Galán-Martín, Á., Tulus, V., and Guillén-Gosálbez, G. (2023). Level of decoupling between economic growth and environmental pressure on earth-system processes. *Sustainable Production and Consumption*, 43:217–229. https://doi.org/10.1016/j.spc.2023.11.001.

[Vea et al., 2020] Vea, E. B., Ryberg, M., Richardson, K., and Hauschild, M. Z. (2020). Framework to define environmental sustainability boundaries and a review of current approaches. *Environmental Research Letters*, 15(10):103003. https://iopscience.iop.org/article/10.1088/1748-9326/abac77/meta.

[Yang and Paulillo, 2026] Yang, Q. and Paulillo, A. (2026). Quantifying environmental impacts on planetary boundaries: A refined and validated impact assessment method. *Environmental Impact Assessment Review*, 119:108355. https://doi.org/10.1016/j.eiar.2026.108355 (accessed May 2026).

[Zhai et al., 2018] Zhai, P., Pörtner, H., Roberts, D., Skea, J., Shukla, P., Pirani, A., Moufouma-Okia, W., Péan, C., Pidcock, R., Connors, S., et al. (2018). Global warming of 1.5° c. an ipcc special report on the impacts of global warming of 1.5° c above pre-industrial levels and related global greenhouse gas emission pathways, in the context of strengthening the global response to the threat of climate change. *Sustainable development, and efforts to eradicate poverty*, 32.